



# International Agreement Report

## RELAP5, TRACE and APROS Model Benchmark for the IAEA SPE-2 Experiment

Prepared by:  
R. Orosz, T. Varju, Á. Aranyosy, V. Holl, T. Hajas & A. Aszódi

Budapest University of Technology and Economics  
Institute of Nuclear Techniques  
Műgyetem rkp. 3.  
1111 Budapest, Hungary

K. Tien, NRC Project Manager

**Division of Systems Analysis**  
**Office of Nuclear Regulatory Research**  
**U.S. Nuclear Regulatory Commission**  
Washington, DC 20555-0001

**Manuscript Completed:** June 2023  
**Date Published:** March 2024

Prepared as part of  
The Agreement on Research Participation and Technical Exchange  
Under the Thermal-Hydraulic Code Applications and Maintenance Program (CAMP)

**Published by**  
**U.S. Nuclear Regulatory Commission**

## AVAILABILITY OF REFERENCE MATERIALS IN NRC PUBLICATIONS

### NRC Reference Material

As of November 1999, you may electronically access NUREG-series publications and other NRC records at NRC's Library at [www.nrc.gov/reading-rm.html](http://www.nrc.gov/reading-rm.html). Publicly released records include, to name a few, NUREG-series publications; *Federal Register* notices; applicant, licensee, and vendor documents and correspondence; NRC correspondence and internal memoranda; bulletins and information notices; inspection and investigative reports; licensee event reports; and Commission papers and their attachments.

NRC publications in the NUREG series, NRC regulations, and Title 10, "Energy," in the *Code of Federal Regulations* may also be purchased from one of these two sources.

#### 1. The Superintendent of Documents

U.S. Government Publishing Office  
Washington, DC 20402-0001  
Internet: <https://bookstore.gpo.gov/>  
Telephone: (202) 512-1800  
Fax: (202) 512-2104

#### 2. The National Technical Information Service

5301 Shawnee Road  
Alexandria, VA 22312-0002  
Internet: <https://www.ntis.gov/>  
1-800-553-6847 or, locally, (703) 605-6000

A single copy of each NRC draft report for comment is available free, to the extent of supply, upon written request as follows:

Address: **U.S. Nuclear Regulatory Commission**  
Office of Administration  
Digital Communications and Administrative  
Services Branch  
Washington, DC 20555-0001  
E-mail: [Reproduction.Resource@nrc.gov](mailto:Reproduction.Resource@nrc.gov)  
Facsimile: (301) 415-2289

Some publications in the NUREG series that are posted at NRC's Web site address [www.nrc.gov/reading-rm/doc-collections/nuregs](http://www.nrc.gov/reading-rm/doc-collections/nuregs) are updated periodically and may differ from the last printed version. Although references to material found on a Web site bear the date the material was accessed, the material available on the date cited may subsequently be removed from the site.

### Non-NRC Reference Material

Documents available from public and special technical libraries include all open literature items, such as books, journal articles, transactions, *Federal Register* notices, Federal and State legislation, and congressional reports. Such documents as theses, dissertations, foreign reports and translations, and non-NRC conference proceedings may be purchased from their sponsoring organization.

Copies of industry codes and standards used in a substantive manner in the NRC regulatory process are maintained at—

#### The NRC Technical Library

Two White Flint North  
11545 Rockville Pike  
Rockville, MD 20852-2738

These standards are available in the library for reference use by the public. Codes and standards are usually copyrighted and may be purchased from the originating organization or, if they are American National Standards, from—

#### American National Standards Institute

11 West 42nd Street  
New York, NY 10036-8002  
Internet: [www.ansi.org](http://www.ansi.org)  
(212) 642-4900

Legally binding regulatory requirements are stated only in laws; NRC regulations; licenses, including technical specifications; or orders, not in NUREG-series publications. The views expressed in contractor prepared publications in this series are not necessarily those of the NRC.

The NUREG series comprises (1) technical and administrative reports and books prepared by the staff (NUREG-XXXX) or agency contractors (NUREG/CR-XXXX), (2) proceedings of conferences (NUREG/CP-XXXX), (3) reports resulting from international agreements (NUREG/IA-XXXX), (4) brochures (NUREG/BR-XXXX), and (5) compilations of legal decisions and orders of the Commission and Atomic and Safety Licensing Boards and of Directors' decisions under Section 2.206 of NRC's regulations (NUREG-0750), and (6) Knowledge Management prepared by NRC staff or agency contractors.

**DISCLAIMER:** This report was prepared under an international cooperative agreement for the exchange of technical information. Neither the U.S. Government nor any agency thereof, nor any employee, makes any warranty, expressed or implied, or assumes any legal liability or responsibility for any third party's use, or the results of such use, of any information, apparatus, product or process disclosed in this publication, or represents that its use by such third party would not infringe privately owned rights.



# International Agreement Report

## RELAP5, TRACE and APROS Model Benchmark for the IAEA SPE-2 Experiment

Prepared by:  
R. Orosz, T. Varju, Á. Aranyosy, V. Holl, T. Hajas & A. Aszódi

Budapest University of Technology and Economics  
Institute of Nuclear Techniques  
Műegyetem rkp. 3.  
1111 Budapest, Hungary

K. Tien, NRC Project Manager

**Division of Systems Analysis  
Office of Nuclear Regulatory Research  
U.S. Nuclear Regulatory Commission  
Washington, DC 20555-0001**

**Manuscript Completed:** June 2023  
**Date Published:** March 2024

Prepared as part of  
The Agreement on Research Participation and Technical Exchange  
Under the Thermal-Hydraulic Code Applications and Maintenance Program (CAMP)

**Published by  
U.S. Nuclear Regulatory Commission**



## ABSTRACT

In the recent decades, with the ever-growing computational capacity, system codes have become essential tools at research and development activities, assessments and licencing procedures of NPPs and research reactors. Among others, a broad literature of assessments performed with RELAP5 and TRACE codes is now available, proving the reliability of the produced results.

In one of our previous studies, dealing with the IAEA SPE-4 benchmark test, we evaluated and compared our simulation results of multiple system codes, namely RELAP5, TRACE and the Finnish APROS. The current study could be considered as the continuation of the mentioned one, as both tests were conducted on the PMK-2 integral test facility in Budapest, Hungary. Although both benchmarks are dealing with a CL-SBLOCA transient, there are several key differences greatly influencing the transient behaviour, such as the availability of emergency core cooling systems (ECCS) or the secondary side bleed and feed operation.

As there are significantly less studies dealing with this particular test and those available resulted, on average, in lower accuracy compared to those of the SPE-4, we decided to investigate it simultaneously with three system codes: RELAP5, TRACE and APROS. The results have been evaluated qualitatively and quantitatively through FFTBM and SARBM methods.



# TABLE OF CONTENTS

<b>ABSTRACT</b> .....	<b>iii</b>
<b>TABLE OF CONTENTS</b> .....	<b>v</b>
<b>LIST OF FIGURES</b> .....	<b>vii</b>
<b>LIST OF TABLES</b> .....	<b>ix</b>
<b>ACKNOWLEDGEMENTS</b> .....	<b>xi</b>
<b>ABBREVIATIONS AND ACRONYMS</b> .....	<b>xiii</b>
<b>1 INTRODUCTION</b> .....	<b>1</b>
<b>2 THE SPE-2 INTERNATIONAL BENCHAMRK TEST</b> .....	<b>3</b>
<b>3 SIMULATION MODELS CONSTRUCTED FOR THE SPE-2 EXPERIMENT</b> .....	<b>5</b>
3.1 New RELAP5 Model.....	5
3.2 New TRACE Model.....	7
3.3 New APROS Model.....	9
3.4 Steady-State Parameters .....	11
<b>4 QUALITATIVE EVALUATION OF THE SIMULATIONS</b> .....	<b>13</b>
<b>5 QUALITATIVE SENSITIVITY ANALYSIS OF THE CALCULATIONS</b> .....	<b>21</b>
5.1 RELAP5 Results.....	22
5.2 TRACE Results.....	25
5.3 APROS Results.....	28
<b>6 QUANTITATIVE EVALUATION OF THE MODELS</b> .....	<b>31</b>
6.1 Handling of Reference Water Levels in the Quantitative Methods.....	31
6.2 Evaluation of the Alternative Model Versions .....	36
<b>7 SUMMARY</b> .....	<b>41</b>
<b>8 REFERENCES</b> .....	<b>43</b>





## LIST OF FIGURES

Figure 1-1	Axonometric View of the PMK-2 Facility.....	1
Figure 3-1	RELAP5 Nodalization Scheme of the SPE-2 Experiment.....	6
Figure 3-2	TRACE Nodalization Scheme of the SPE-2 Experiment .....	8
Figure 3-3	APROS Nodalization Scheme of the SPE-2 Experiment.....	9
Figure 4-1	Primary Pressure (PR21) .....	14
Figure 4-2	Mass Flow of the Break Simulator (FL00) .....	15
Figure 4-3	RPV Coolant Level (LE11) .....	15
Figure 4-4	Secondary Pressure (PR81) .....	16
Figure 4-5	CL Loop-Seal Water Level (LE46) .....	17
Figure 4-6	HA2 Coolant Level (LE92) .....	17
Figure 4-7	HL Loop-Seal Coolant Level (LE31).....	18
Figure 4-8	DC Coolant Level (LE61) .....	18
Figure 4-9	Heater Rod Cladding Temperature (TE15).....	19
Figure 5-1	DC Top Region Modeling – RELAP5 .....	22
Figure 5-2	Primary Pressure – RELAP5 Calculations.....	23
Figure 5-3	HA1 Coolant Level – RELAP5 Calculations .....	23
Figure 5-4	DC Coolant Level – RELAP5 Calculations .....	23
Figure 5-5	Mixture Mass Flow of the Break Valve – RELAP5 Calculations.....	23
Figure 5-6	RPV Coolant Level – RELAP5 Calculations .....	24
Figure 5-7	HL Loop-Seal Level – RELAP5 Calculations.....	24
Figure 5-8	Secondary Pressure – RELAP5 Calculations.....	24
Figure 5-9	DC Top Region Modeling – TRACE.....	25
Figure 5-10	HL Loop-Seal Level – TRACE Calculations .....	26
Figure 5-11	Primary Pressure – TRACE Calculations .....	26
Figure 5-12	HA1 Coolant Level – TRACE Calculations.....	26
Figure 5-13	RPV Coolant Level – TRACE Calculations.....	27
Figure 5-14	DC Coolant Level – TRACE Calculations.....	27
Figure 5-15	Mixture Mass Flow of the Break Valve – TRACE Calculations .....	27
Figure 5-16	HA1 Coolant Level – APROS Calculations.....	28
Figure 5-17	Primary Pressure – APROS Calculations.....	29
Figure 5-18	HL Loop-Seal Level – APROS Calculations .....	29
Figure 5-19	Heater Rod Cladding Temperature – APROS Calculations.....	29
Figure 6-1	Time-Dependent Accuracy of the UP Pressure (FFTBM-SM) .....	36

Figure 6-2	Time-Dependent Accuracy of the UP Pressure (SARBM) .....	36
Figure 6-3	Time-Dependent Total Accuracy of the Base Calculations (SARBM) .....	37
Figure 6-4	Time-Dependent Total Accuracy of the Base Calculations (FFTBM-SM) .....	37
Figure 6-5	Time-Dependent Total Average Accuracy of the Alternative TRACE Model Versions .....	37
Figure 6-6	Time-Dependent Total Average Accuracy of the Alternative RELAP5 Model Versions .....	37
Figure 6-7	Time-Dependent Total Average Accuracy of the Alternative APROS Model Versions .....	38

## LIST OF TABLES

Table 2-1	Main Features of the SPE-2 and SPE-4 Tests .....	3
Table 3-1	Discharge Coefficients for Choked Flow Modeling .....	5
Table 3-2	Steady-State Performance of the Models.....	11
Table 4-1	Sequence of Major Events .....	13
Table 5-1	Base and Alternative Model Versions.....	21
Table 6-1	Accuracy Categories of FFTBM and SARBM.....	31
Table 6-2	Parameter Set for the Quantitative Methods .....	32
Table 6-3	Accuracy Measures for SIT2 Water Level Calculations .....	32
Table 6-4	FFTBM-SM Quantification of Water Level Measurements based on 'Absolute' and 'Relative' Reference Points .....	33
Table 6-5	SARBM Quantification of Water Level Measurements based on 'Absolute' and 'Relative' Reference Points .....	34
Table 6-6	Comparison of Total Accuracies between the Codes and Alternatives (Relative Reference Points) .....	35
Table 6-7	Primary Pressure Accuracies for Base Models .....	35



## **ACKNOWLEDGMENTS**

We would like to acknowledge and give warm thanks József Bánáti (Paks II. Ltd., Hungary) for providing us constant support during the work. His experience helped us a lot during the model development phase and the evaluation of the results.

Also, we would not have been able to perform the quantitative analysis without Dr. Andrej Prošek (JSI, Ljubljana, Slovenia) giving us access to the Excel add-on specifically developed for FFTBM-SM and SARBM calculations. Many thanks for the resources and information regarding their usage.



## ABBREVIATIONS AND ACRONYMS

AA	Average Amplitude
AF	Accuracy Factor
BME	Budapest University of Technology and Economics
CAMP	Code Application and Maintenance Program
CCFL	Countercurrent Flow Limitation
CL	Cold Leg
CRIP	Central Research Institute for Physics
DC	Downcomer
ECCS	Emergency Core Cooling System
EFW	Emergency Feed Water
FFTBM-SM	Fast Fourier Transform Based Method with Signal Mirroring
HA	Hydroaccumulator
HL	Hot Leg
HPIS	High Pressure Injection System
IAEA	International Atomic Energy Agency
JSI	Jožef Stefan Institute
NTI	Institute of Nuclear Techniques
PMK	Paksi Modell Kísérlet (in Hungarian)
PWR	Pressurized Water Reactor
RPV	Reactor Pressure Vessel
SARBM	Stochastic Approximation Ratio Based Method
SBLOCA	Small-Break Loss of Coolant Accident
SIT	Safety Injection Tank
SG	Steam Generator
SPE	Standard Problem Exercise
UH	Upper Head
UP	Upper Plenum
US NRC	United States Nuclear Regulatory Commission
WF	Weighting Factor(s)





# 1 INTRODUCTION

In recent years, our Institute (BME NTI) has gained relevant experience with the RELAP5 and TRACE system codes through the CAMP agreement program. The codes issued by the United States Nuclear Regulatory Commission (US NRC) has been used for both educational and research purposes, which resulted in a few studies, reports [1] and articles [2], [3].

Our previous International Agreement Report (NUREG/IA-0533) was dealing with the fourth IAEA Standard Problem Exercise (SPE-4) benchmark, which has been carried out on the PMK-2 facility (Figure 1-1), located in Budapest, Hungary, in the 1990s. In the study, we analysed the test with three different system codes simultaneously, namely with RELAP5, TRACE and the APROS code, the latter of which has been used for many years in the Institute. Comparing our simulation results to the measured datasets and to each other proved to be useful at SPE-4 [1], therefore we decided to follow the same approach with the SPE-2 experiment, which was conducted on the PMK-2 facility as well. For this purpose, our previous models served as a solid base.

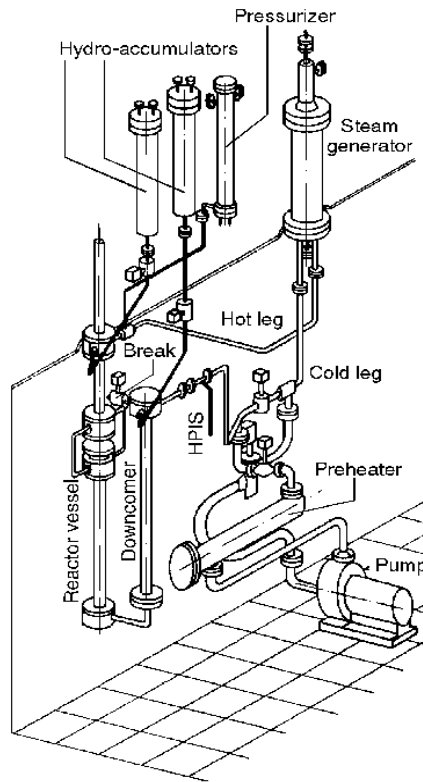


**Figure 1-1 Axonometric View of the PMK-2 Facility**

The second SPE (1987), despite being fairly similar to the fourth one, has generated a rather lower interest among the professionals, according to the available literature. Moreover, generally the professionals reported less accurate predictions in case of the SPE-2 [4], [5], [6], than that of the SPE-4 [7], [8], [1], according to the available studies. The reason could perhaps be an unforeseen difficulty level of producing satisfying simulation results. Besides reproducing the main processes taking place in the reactor in a satisfying manner, we also make an attempt to determine the possible stems of such a difference between the experiments. In order to be consistent with the previous study, the quantitative assessment has been performed again with

the improved Fast Fourier Transform Based Method (FFTBM-SM) and the Stochastic Approximation Ratio Based Method (SARBM).

The report first briefly introduces the PMK-2 integral test facility and the differences between SPE-2 and SPE-4 experiments. Then, the main modifications, needed for the customization of our previous models (presented in [1] in details) for the experiment under investigation, are summarized. Following the qualitative analysis of the main processes, a detailed quantitative assessment, together with the sensitivity analysis of some chosen parameters, is presented.

## 2 THE SPE-2 INTERNATIONAL BENCHAMRK TEST

The second SPE deals with a cold leg small break loss-of-coolant accident (CL-SBLOCA), performed on the PMK-2 integral test facility, which is located at the Central Research Institute for Physics (CRIP) in Budapest, Hungary. The facility served as one of the first full-pressure and full-temperature models of the VVER-440/213 type pressurized water reactors (PWR). It consisted of a single loop, with a power and volume scaling ratio of 1:2070 and the same elevations as those of the reference power plant (practically everywhere across the facility). Equipped with the proper measurement and control system, the design is suitable to investigate the system response to a wide range of transients.

As such, the SBLOCAs conducted on PMK-2 are of significant importance, especially due to some special arrangements of the Russian-type PWRs (e.g., horizontal steam generator, cold and hot leg loop seals, hexagonal fuel bundle). The experiment under investigation, similarly to the SPE-4, features a small cold leg break, located at the top of the external downcomer. In Table 2-1, we summarized the most important features of the two experiments, including the main differences between them.

**Table 2-1 Main Features of the SPE-2 and SPE-4 Tests**

	<b>SPE-2</b>	<b>SPE-4</b>
Experiment commenced from nominal state	✓	✓
Break size (diameter)	3.0 mm	3.2 mm
Pump coast-down & decay power simulated in a prescribed manner	✓	✓
Passive ECCS, no. of hydroaccumulators involved	2	2
High pressure injection system (HPIS)	✓	X
Low pressure injection system (LPIS)	X	✓
Secondary side isolation after the transient initiation	✓	✓
Secondary side bleed operation	X	✓
Emergency feedwater (EFW) injection	X	✓

More detailed information on the facility itself and the experiments can be found in [9] and [10].



### 3 SIMULATION MODELS CONSTRUCTED FOR THE SPE-2 EXPERIMENT

As mentioned before, the models of our previous study [1], built specifically for the SPE-4 benchmark, provided a solid base for our current models. Besides the common features of the experiments, however, there are numerous differences, which had to be taken into account. In the followings, we list the common changes, which had to be implemented in more-or-less the same way in the codes and then we present the most important code-specific modifications necessary.

Due to the minor differences in steady-state conditions, we had to adjust the values of nominal parameters, such as the primary and secondary pressures, water levels and the coolant mass flows. Then, the required heat loss distribution and the pressure differences have been achieved through the appropriate heat transfer and loss coefficients. Obviously, some pivotal components (ECCS, EFW, etc.) had to be added, modified, or deleted/deactivated, as listed in Table 2-1. The transient initiation is also followed by different interventions of the control system, including valve opening/closure and SCRAM setpoints, pump coastdown timing, etc. In order to be in compliance with the experiment, the decay heat curve and some boundary conditions (e.g., the back-pressure boundary) were also modified in the models.

Best overall agreement has been achieved with the Henry-Fauske critical flow model in case of RELAP5, contrary to the SPE-4 experiment [1], where the Ransom-Trapp model seemed to perform better. The new discharge coefficients for both subcooled and two-phase & superheated regions applied at relief and break valves are summarized in Table 3-1.

**Table 3-1 Discharge Coefficients for Choked Flow Modeling**

	BREAK VALVE		RELIEF VALVE	
	Subcooled	Two-phase & superheated	Subcooled	Two-phase & superheated
<b>RELAP5</b>	1.05	1.05	0.7	0.7
<b>TRACE</b>	0.9	1.0	0.6	0.6
<b>APROS</b>	0.9	0.9	0.55	0.55

In addition to the common changes, some specific modifications had to be implemented in the different codes.

#### **3.1 New RELAP5 Model**

Throughout the model development, many versions have been built and the modelling of the dynamic two-phase processes at break surroundings appeared to be the most challenging task, as many pipe sections connect in a rather small volume, the downcomer top. In the RELAP5 model (Figure 3-1), both the surge line of SIT1 (safety injection tank) and the break line connections have been placed slightly higher than that of the cold leg (contrary to the geometry of the facility, where all 3 connections share the same elevation). This modification, among others, is further discussed in Chapter 5, as part of a smaller-scale sensitivity analysis of the models. Formerly, our RELAP5 model was not equipped with the pressure limitation function of valve PV23 (see Figure 3-1), because the opening pressure setpoint has not been reached throughout the transient of SPE-4, but the SPE-2 model already features it.

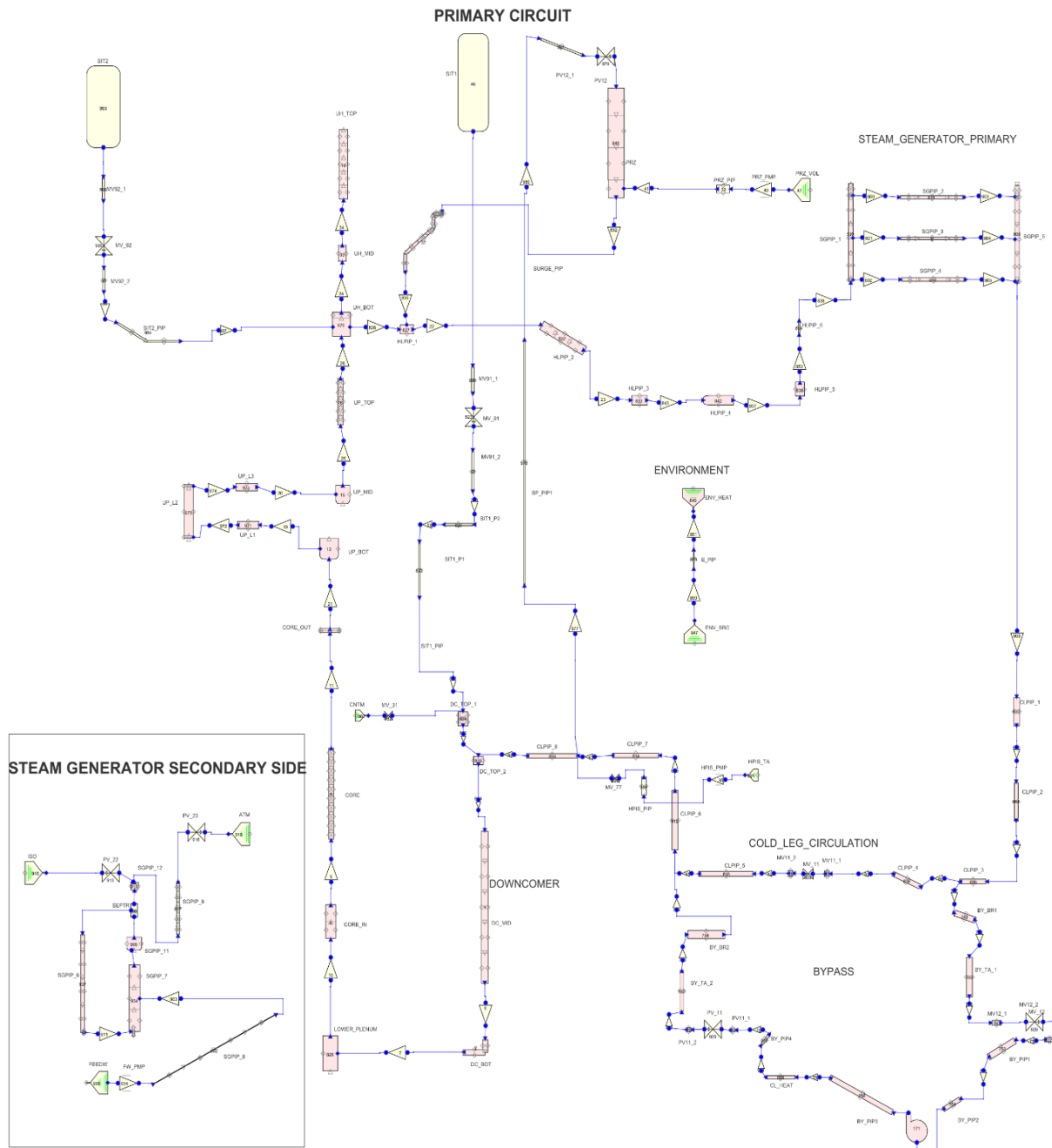


Figure 3-1 RELAP5 Nodalization Scheme of the SPE-2 Experiment

## **3.2 New TRACE Model**

Slight modifications have been applied regarding the downcomer top connections in TRACE as well, namely, the SIT1 surge connection has been elevated by 9.65 cm (now connecting to the uppermost node of the downcomer, as seen in Figure 3-2). The effect of this change will be discussed later in Chapter 5 and 6.

The nodalization of the steam generator (SG) has also been redesigned; a finer nodalization of the collectors allowed the repositioning of the heat exchanger tubes in a way that the upper- and lowermost tubes in the model are the same elevation as those in the facility. This setup is believed to simulate the flow-through more accurately by lower water levels in the collectors. In addition, the crossflow connections have been removed in the secondary side between the SG riser chamber and the downcomer because of occasional stability issues.

Due to the complete isolation of secondary side during the transient, the steam line (to valve PV23, see in [1]) has little to no influence on the secondary side; therefore, the model has been simplified with it.

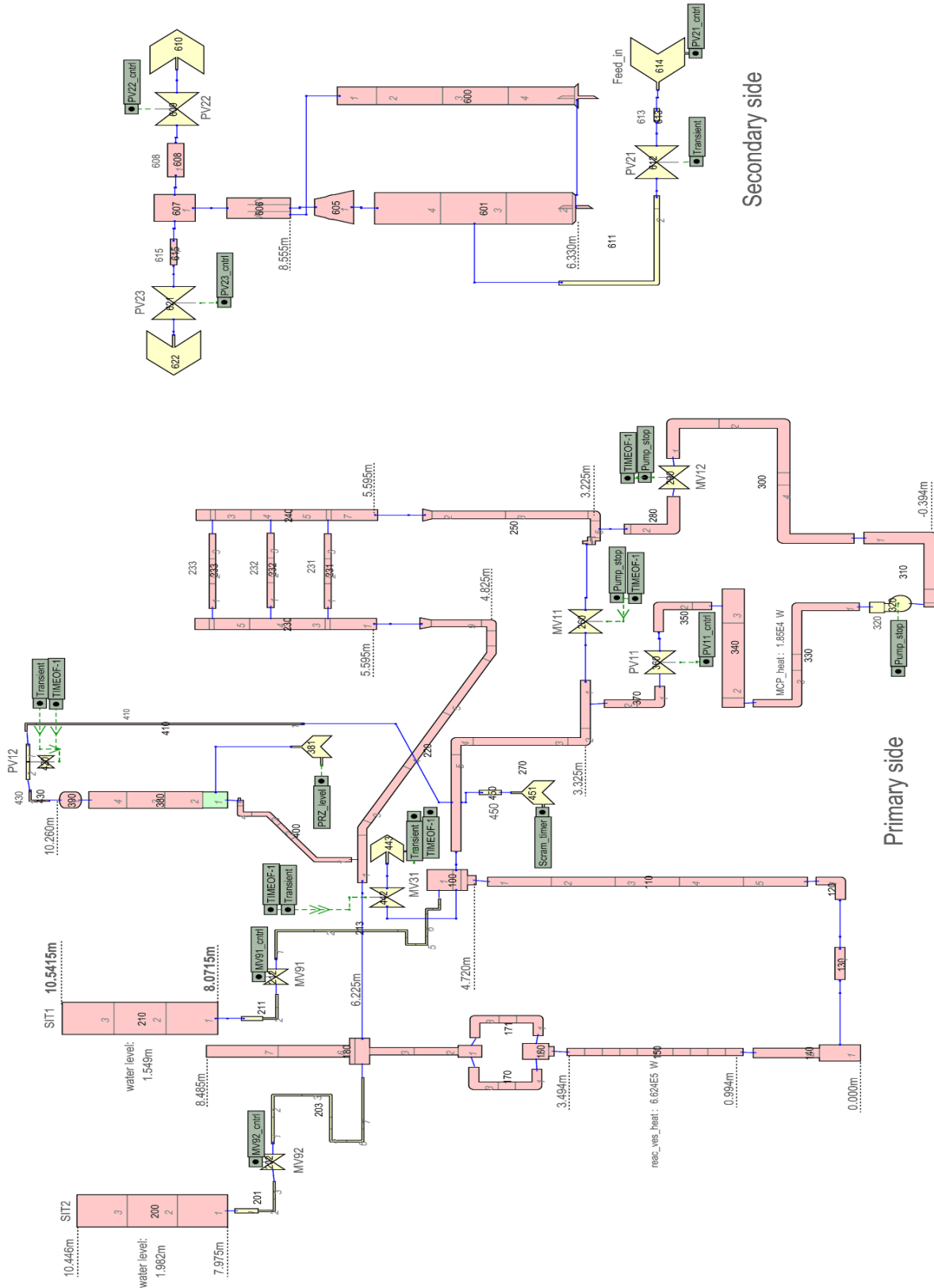


Figure 3-2 TRACE Nodalization Scheme of the SPE-2 Experiment



### 3.3 New APROS Model

Similarly to TRACE, a simplification has been implemented at the main wall steam pipeline; moreover, the upper part of SG has been renodalized and the formerly used recirculation branch has been removed (Figure 3-3).

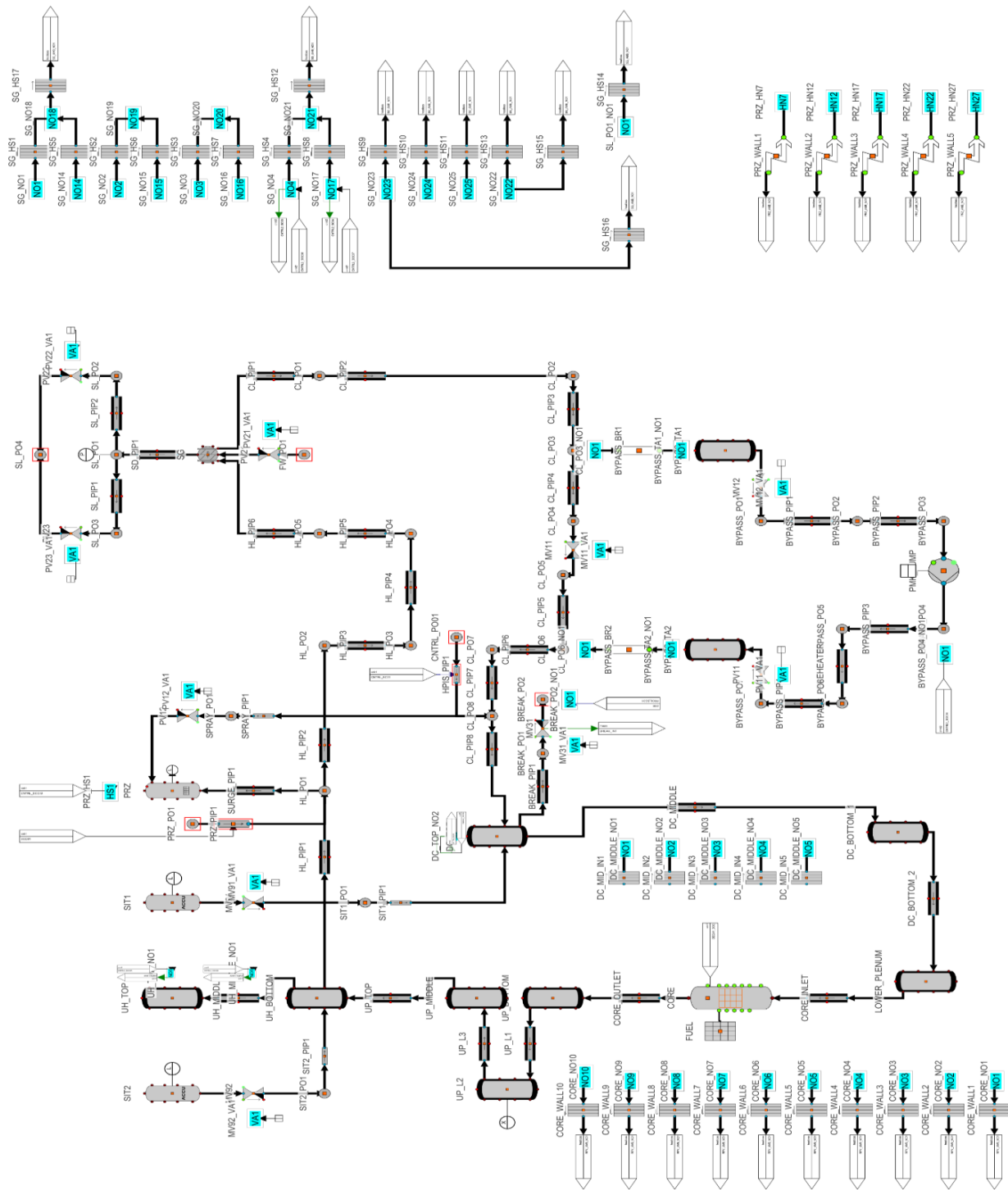


Figure 3-3 APROS Nodalization Scheme of the SPE-2 Experiment

Based on our previous experiences, the built-in accumulator model of APROS does not predict well the injection rates in some cases when using default parameters. As discussed in [1], an accurate prediction requires the adjustment of the heat transfer between the phases through an 'efficiency factor', ranging from 0 to infinite, i.e., the calculated heat transfer is increased, when the multiplier is larger than 1 and decreased otherwise. In case of the SPE-4 experiment, we obtained the best results by setting the multipliers to 5.0 in both hydroaccumulators, which had to be adjusted at SPE-2 to 3.5 and 3.0 in SIT1 and SIT2, respectively. In the sensitivity analysis of the APROS model, among others, the effect of using the default HA settings on the simulation accuracy is shown.

### 3.4 Steady-State Parameters

In order to assure proper initial conditions for the transient, numerous actions were implemented. Besides setting the correct setpoints, power, coolant levels and mass flow rates, the changed heat loss distribution and pressure differentials were also considered. Table 3-2 shows the comparison of the most important steady-state parameters.

It can be seen that most of the parameters meet or fall slightly out of the measurement uncertainty intervals. Two specific parameters have to be commented on: First, the measured primary pressure (PR21) value listed in the table has been taken from the CD appendix of the book [11], while the PI controller has been set to 12.18 MPa (as stated in [9]) in the models. Secondly, a rather strange behavior could be discovered in the measured values, as the coolant temperature in the SG inlet is 2 K higher than that of the upper plenum. Since there is no heat source in between the two measurement points, one may assume that the measured data (TE41) is inaccurate. The simulation results, otherwise, uniformly show a 0.3-0.4 K temperature drop between the two points under investigation.

**Table 3-2 Steady-State Performance of the Models**

Parameter	ID	Unit	Measurement	RELAP5	TRACE	APROS
Primary pressure (UP)	PR21	MPa	12.14 ± 0.05	12.07	12.17	12.18
Secondary pressure	PR81	MPa	5.07 ± 0.02	5.07	5.07	5.07
Primary mass flow rate (CL)	FL53	kg/s	4.60 ± 0.06	4.60	4.60	4.60
Lower plenum inlet temperature	TE63	K	546.5 ± 1.0	546.4	545.8	545.2
Upper plenum temperature	TE22	K	573.9 ± 1.0	573.4	572.9	572.5
SG inlet coolant temperature	TE41	K	575.9 ± 1.0	573.2	572.5	572.1
SG outlet coolant temperature	TE42	K	545.3 ± 1.0	545.1	545.5	544.9
SG collapsed level (secondary side)	LE81	m	7.99 ± 0.05	7.99	7.99	7.99
Pressurizer water level	LE71	m	9.40 ± 0.02	9.40	9.40	9.40
SIT1 water level	LE91	m	9.52 ± 0.02	9.52	9.52	9.52
SIT2 water level	LE92	m	9.96 ± 0.02	9.95	9.96	9.96
Fuel rod simulator power	PW01	kW	662.4 ± 3.0	662.4	662.4	662.4

The achieved proper steady-state conditions enabled us the thorough investigation of the SBLOCA transient, the assessment of which is presented in the following chapters.



## 4 QUALITATIVE EVALUATION OF THE SIMULATIONS

This section summarizes and compares the main processes taking place in the system with those estimated by the best performing code models. It has to be clarified therefore, that each time the codes (e.g., 'TRACE', 'RELAP5', 'APROS') are mentioned, we refer to the accuracy of the actual model (encompassing user effect, nodalization, etc.). Figures 4-1 to 4-9 were chosen to facilitate the understanding of the relevant processes discussed. Also, the sequence of major events is presented in Table 4-1.

**Table 4-1 Sequence of Major Events**

	Measurement (SPE-2)	RELAP5 calculation	TRACE calculation	APROS calculation
Transient initiation (break)	0 s	0 s	0 s	0 s
SCRAM signal	3 s	2.6 s	2.9 s	1.4 s
Pump coast-down initiation	11 s	15.2 s	13.1 s	4.2 s
Pressurizer empties completely	15 s	15.8 s	12.7 s	52.8 s
Secondary side blow-down initiation	15 s	6.8 s	7.9 s	11.0 s
HA-1 injection start	39 s	42.5 s	90.6 s	38.0 s
HA-2 injection start	38 s	42.5 s	90.6 s	38.0 s
RPV coolant level below hot leg nozzle	60 s	50.9 s	67.0 s	93.0 s
HPIS injection start	63 s	62.6 s	62.9 s	61.4 s
Secondary side blow-down ending	71 s	66.4 s	70.8 s	71.7 s
Reversed core flow occur	185 s	174 s	195 s	191 s
Heat transfer reverses in the SG	200 s	208 s	182 s	199 s
Two-phase break flow dominates	212 s	74.6 s (early) 206 s (permanent)	226 s	250 s
HA-1 injection stop	397 s	478 s	479 s	404 s
HA-2 injection stop	405 s	480 s	422 s	410 s

In the course of the 1000 s long transient 4 stages can be recognized, which are discussed below.

In **Stage 1**, break valve MV31 opens, which starts the CL-SBLOCA transient. First, a sharp drop of the primary pressure can be observed in Figure 4-1 due to the discharged coolant. Once the SCRAM setpoint is reached, numerous control interventions are initiated, such as the electric, heating power reduction and the pump coastdown. The timing of these is well predicted by RELAP5 and TRACE, while APROS calculated a sharper pressure drop, resulting in an earlier SCRAM. Then, the pressure reduction is stalled between around 50 and 210 s due to the intensive boiling taking place in the UH. Figure 4-2 shows, that the mass flow rate through the break is consistently overestimated by the codes throughout the transient, even when the pressure evolution is accurate. The only exemption is shown by TRACE in the above-mentioned period, where it shows roughly the same mass flow rate as measured in the facility. Based on the simulation data, it was clear however, that a rather early voiding was present in the break area in TRACE, which, compared to the other two codes, allowed lower mixture mass flow rates and resulted in a pressure stagnation at a higher pressure level between 50 and 100 s (see Figure 4-1). Taking this into consideration, it can be stated, that generally higher mass flow rates are required in the calculations to achieve an accurate pressure evolution in the primary side. In [9] it has been reported, that, because of some hardships of the density measurements, the mass flows were calculated considering saturated steam conditions, which could possibly explain this discrepancy.

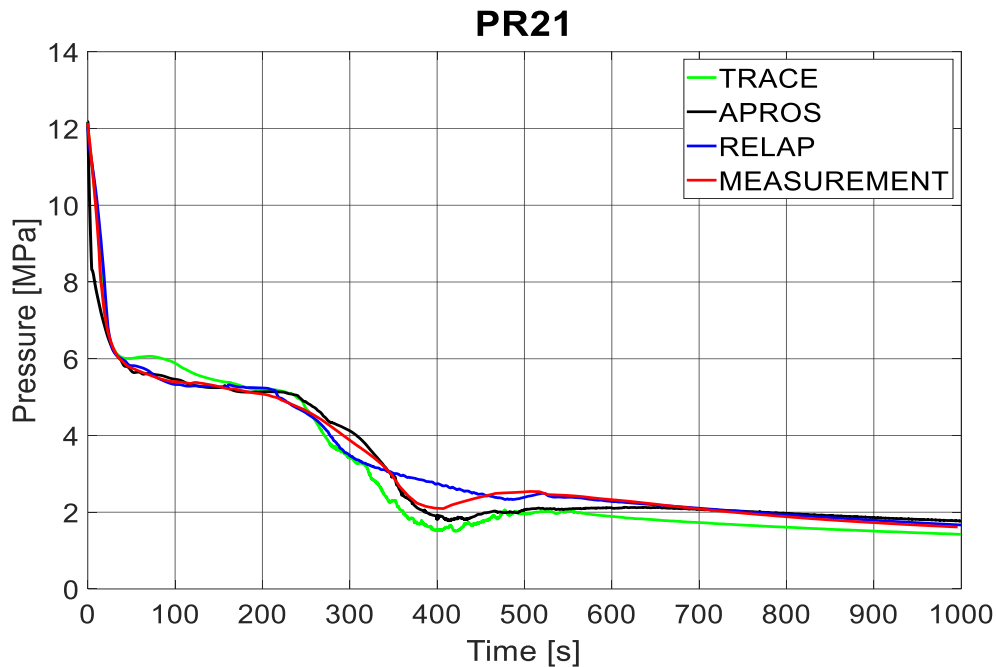


**Figure 4-1 Primary Pressure (PR21)**

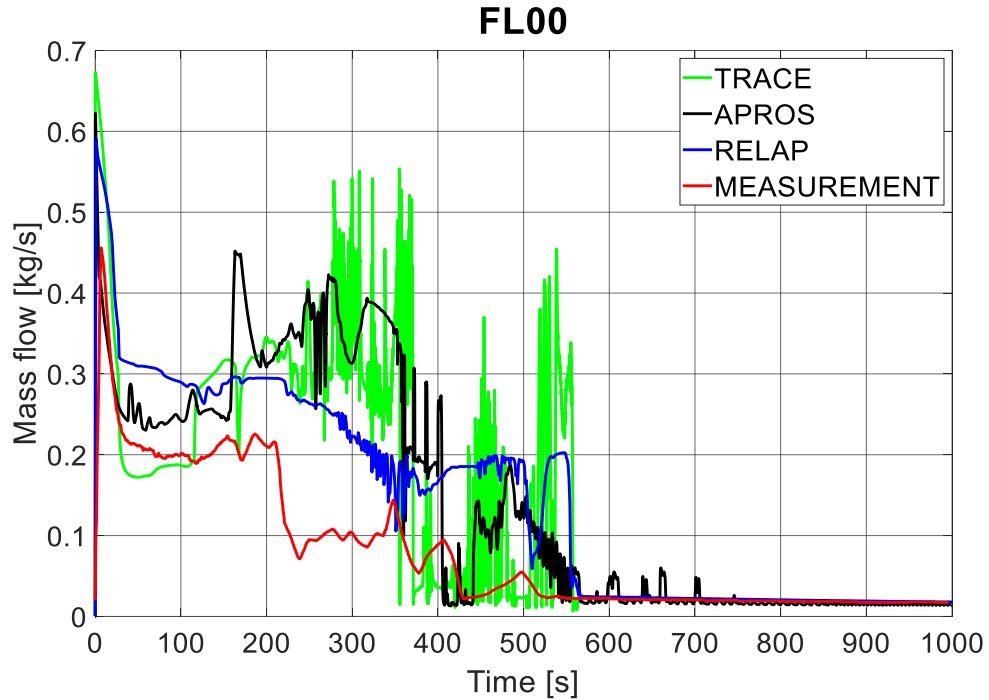


**Figure 4-2 Mass Flow of the Break Simulator (FL00)**

The hydroaccumulators start to inject in the first part of this phase, however, the coolant level in the RPV keeps decreasing (see Figure 4-3). Similar trends of the collapsed levels can be observed in each calculation but resulting in a lower water level at the end of this phase compared to that of the measurement.

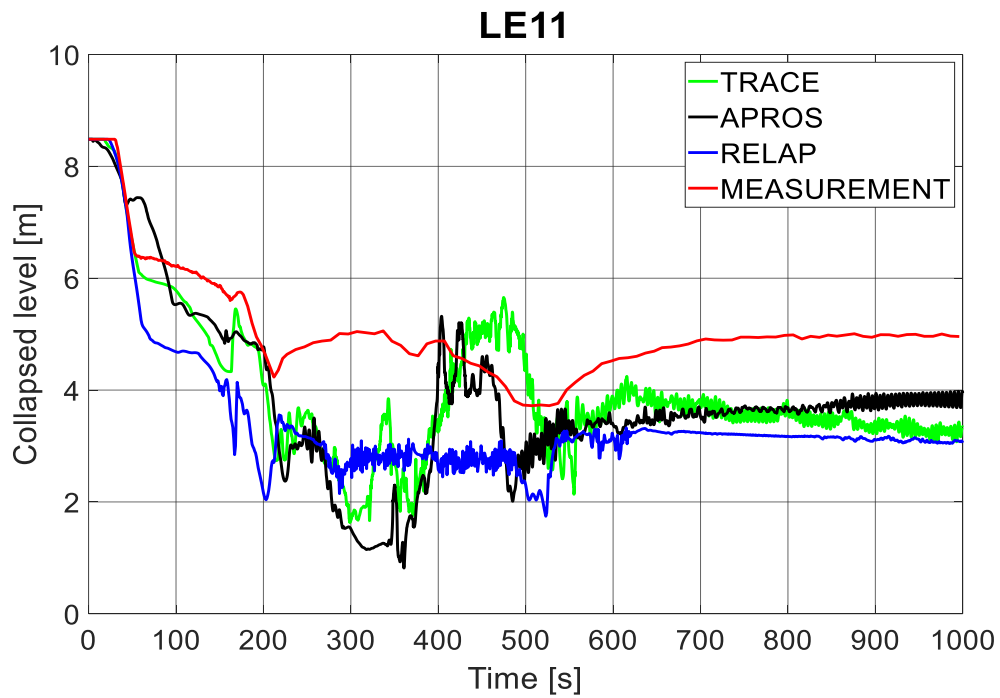


**Figure 4-3 RPV Coolant Level (LE11)**

Meanwhile, the secondary side has been isolated, and the rising pressure reached the pressure limitation onset setpoint of valve PV23. In about 50 s its closure took place and the secondary pressure started to rise again. As seen in Figure 4-4, an accurate timing of the pressure limitation interventions has been achieved by the codes, however, RELAP5 and TRACE overestimated both the first and second pressure peaks, which could stem from the imperfect modelling of heat transfer and heat losses in the secondary side.

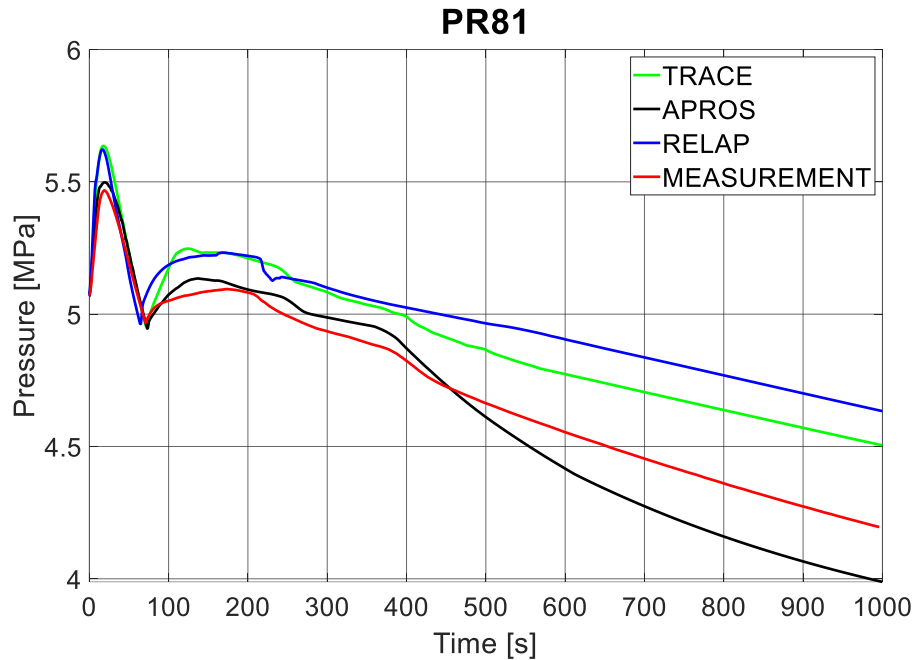


**Figure 4-4 Secondary Pressure (PR81)**

We consider entering into **Stage 2** when the forced convection stops and the bypass loop, containing the MCP, is disconnected by valves PV11 and MV12. So far, the CL loop seal blocked the path of the generated steam, which is emptied however, after around 200 s (Figure 4-5). This allows the further depressurization of the system and therefore higher injection mass flows of the SITs (Figure 4-6). Due to the HA injection, the HL loop seal (Figure 4-7), which emptied during the first phase, fills back up. The timing of this process is quite well predicted by APROS; RELAP5 estimated an earlier refill and TRACE showed a dynamic process, in which the refill process has been interrupted two times by a temporal emptying. In the simulations, TRACE and APROS captured the HA injection characteristics quite well, while in this stage, RELAP5 indicated slower HA injection, which is due to the discrepancy of the governing UP pressure between 250 and 450 s (caused by the HL loop seal behaviour).



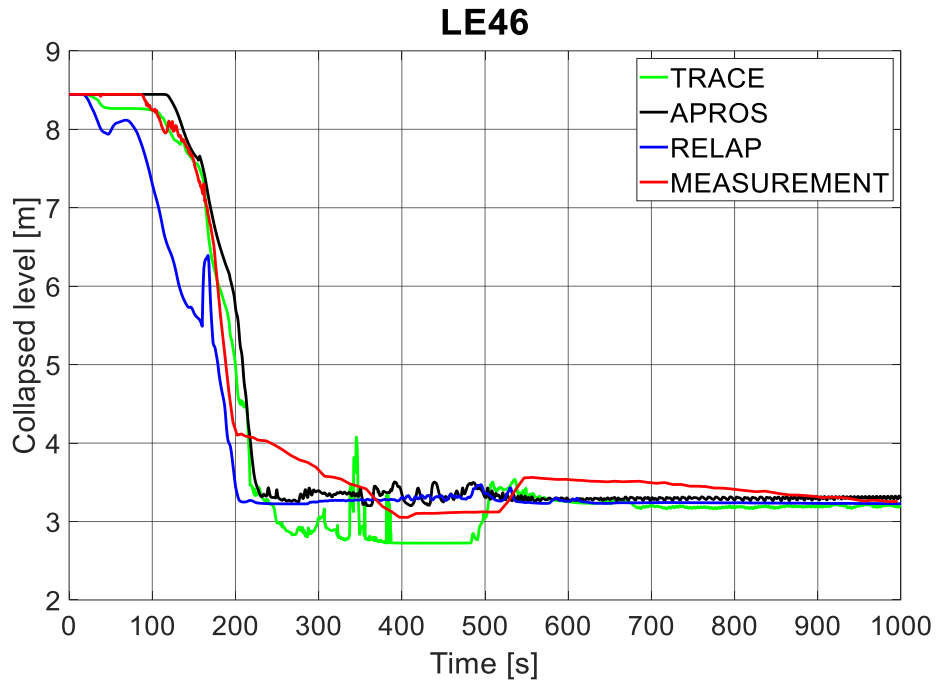


**Figure 4-5 CL Loop-Seal Water Level (LE46)**

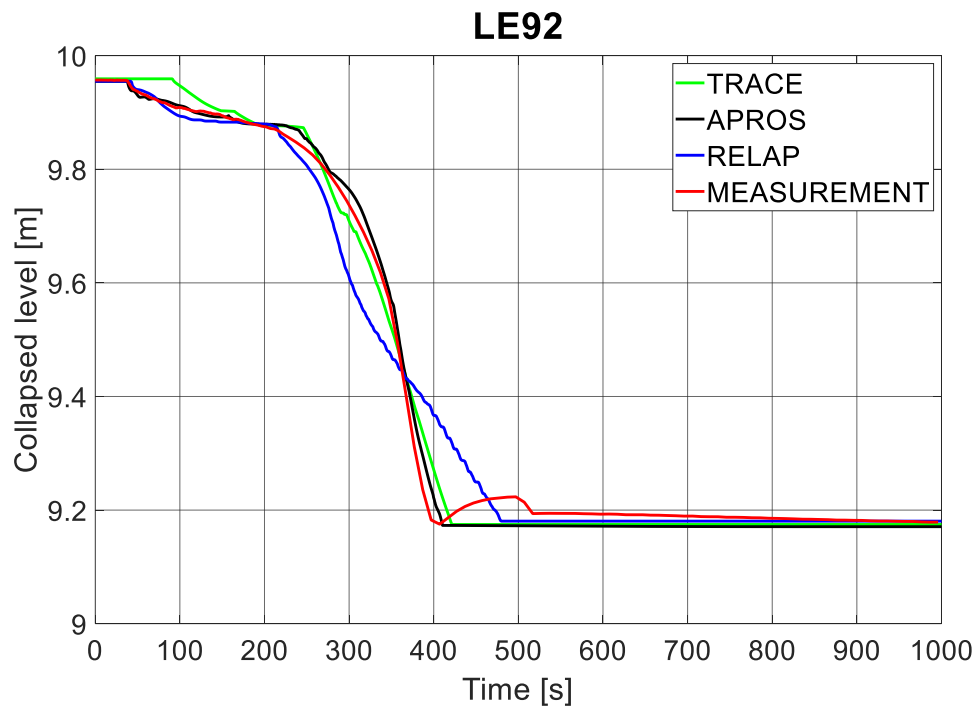


**Figure 4-6 HA2 Coolant Level (LE92)**

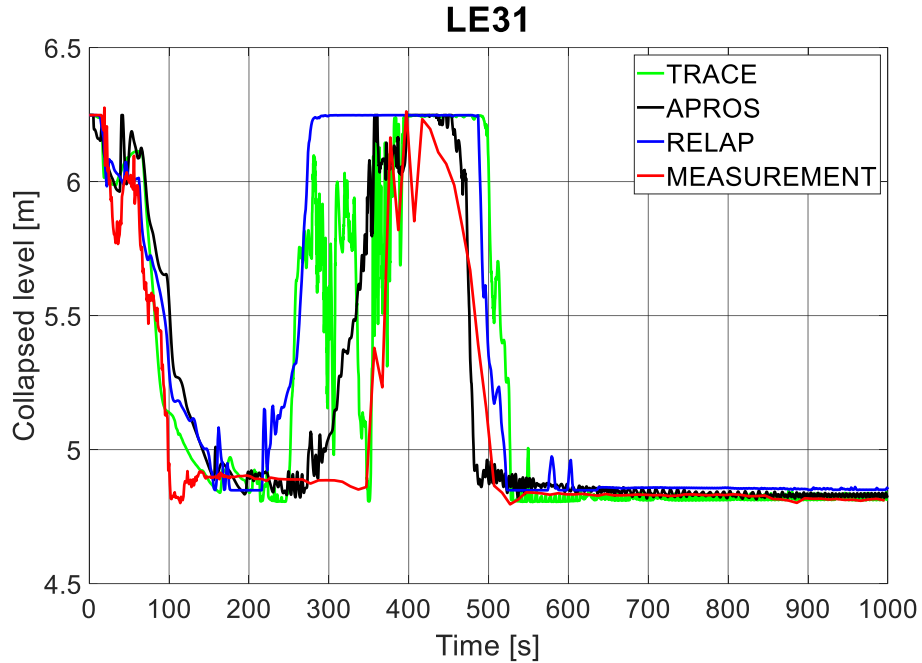


**Figure 4-7 HL Loop-Seal Coolant Level (LE31)**

As a result of the escaping coolant through the break, the DC water level also shows a sharp decrease (Figure 4-8), which has been stopped by the high SIT1 injection rate between around 300 and 400 s. Approximately at the end of the SIT injection, the DCs are completely refilled. The heat transfer in the SG reverses, as the primary pressure drops below that of the secondary side, therefore, PR81 decreases monotonically throughout the rest of the transient.

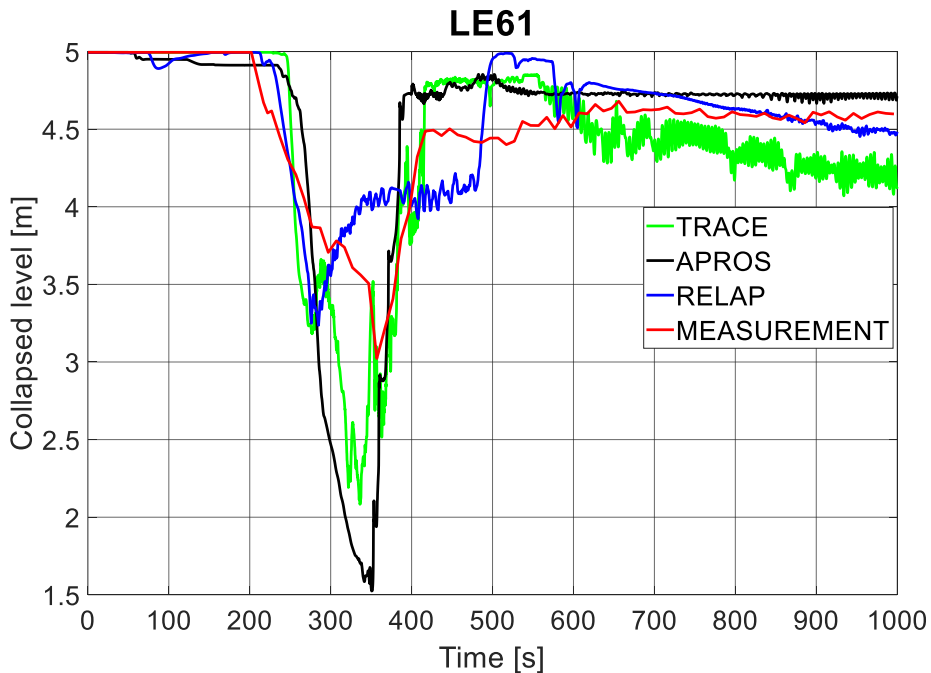


**Figure 4-8 DC Coolant Level (LE61)**

**Stage 3:** As the HL loop seal is refilled, the generated steam in the UP cannot escape through the break, so a temporal pressure increase (Figure 4-1) can be observed until the loop seal clearance (500-550 s). The increasing pressure should result in a decrease of the RPV collapsed water level (as also shown by the measurement). This behaviour can be clearly seen in the TRACE and APROS calculations, while that of the RELAP5 captured it rather moderately, as (due to the slower accumulator injection) a lower coolant level was present in the RPV at the time. As mentioned, the secondary pressure keeps decreasing and its rate indicates the flow characteristics of the primary side, namely the loop seal clearance.

**Stage 4:** After the loop seal clearance there are no further interventions on the system; the single HPIS line provides the water needed for the long-term cooling of the fuel rods (see Figure 4-9). The RPV water level consolidates at the top of the heated section, the code calculations however significantly underestimate it compared to the measurement. This behavior can be observed for the most of the transient, the reason behind of which would need further investigation.

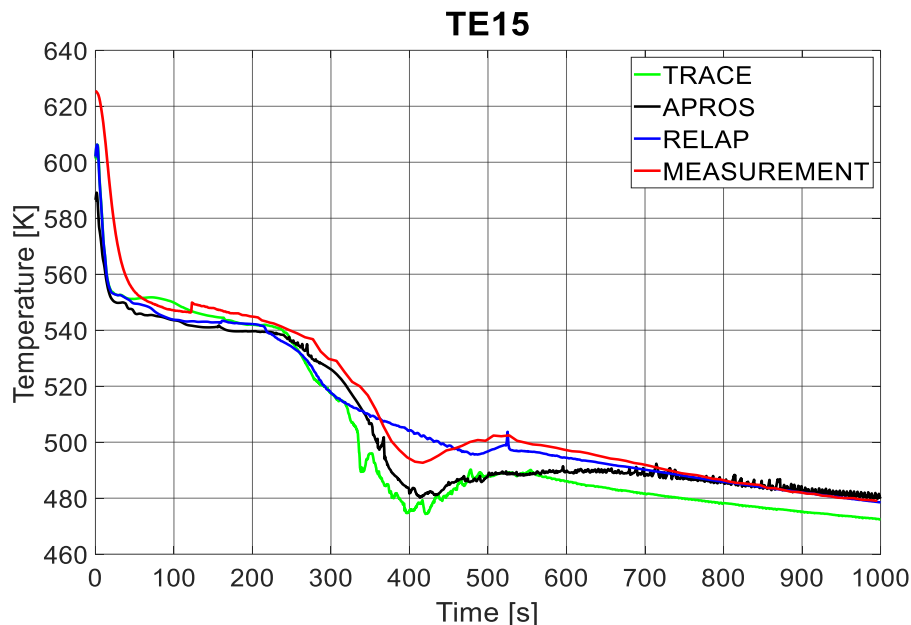


**Figure 4-9 Heater Rod Cladding Temperature (TE15)**

The qualitative evaluation showed that our models captured the most important processes taking place in the reactor. It has been proven, that the available safety systems are capable of handling the posed design basis accident scenario, as the heater rods did not dry out throughout the transient (see Figure 4-9). In most cases, the trends are replicated qualitatively well by the codes, the timing of certain processes are however shifted (HL loop seal refill – RELAP5, TRACE; HA injection rate – RELAP5; DC water level refill – RELAP5). Moreover, the cases of LE11 and FL00 has been mentioned as potential areas of improvement. It has to be mentioned however, that these investigations would require further information/data on the facility, which is more-or-less impossible to acquire, since the experiment was carried out decades ago. From the modelling perspective, the break and its surroundings appeared to be the most challenging. It is a relatively small volume with multiple inlet and outlet connections (HA1, CL, DC, BREAK), in which dynamic two-phase processes take place. Therefore, among others, multiple variants of inlet/outlet positions have been tested in RELAP5 and TRACE,

which of course differ from the original geometry. Without such modifications (only by adjusting the break discharge coefficient), unlike in case of SPE-4, we could not reach sufficient agreement between the simulations and the measured data.

## 5 QUALITATIVE SENSITIVITY ANALYSIS OF THE CALCULATIONS

Those models presented in the previous chapters are the closest to the measurements; therefore, they will be denoted as *Base* from now on. On the other hand, three other alternatives were chosen to be investigated here in RELAP5 and TRACE, while we introduce 1 extra APROS model worth mentioning. Please refer to Table 5-1 for the summary of these model versions.

**Table 5-1 Base and Alternative Model Versions**

	Model version	Description
RELAP5	<i>Base</i>	Two-phase & superheated discharge coeff.: 1.05; modified geometry (see Figure 5-1, A)
	<i>Geom</i>	Two-phase & superheated discharge coeff.: 1.05; original geometry (see Figure 5-1, B)
	<i>Dc</i>	Two-phase & superheated discharge coeff.: 1.00; modified geometry (see Figure 5-1, A)
	<i>Geom_Dc</i>	Two-phase & superheated discharge coeff.: 1.00; realistic geometry (see Figure 5-1, B)
TRACE	<i>Base</i>	Two-phase & superheated discharge coeff.: 1.00; modified geometry (see Figure 5-9, A)
	<i>Geom</i>	Two-phase & superheated discharge coeff.: 1.00; realistic geometry (see Figure 5-9, B)
	<i>Dc</i>	Two-phase & superheated discharge coeff.: 1.01; modified geometry (see Figure 5-9, A)
	<i>Geom_Dc</i>	Two-phase & superheated discharge coeff.: 1.01; realistic geometry (see Figure 5-9, B)
APROS	<i>Modified_HA</i>	Modified 'efficiency factor' (3.5/3.0)
	<i>Default HA</i>	Default 'efficiency factor' (1.0/1.0)

We followed similar strategy for RELAP5 and TRACE, as one alternative (called *Geom*) considers the original geometry of the DC top region (the connections are not varied) with unchanged choked flow multipliers (for the *Reference* values see Table 3-1). The other version (*Dc*) is intended to capture the effect of the adjustment of the discharge coefficient only (applying the same geometry as used in *Base* case). Finally, the *Geom\_Dc* alternative combines the above-mentioned two changes. The APROS model did not tend to be as sensitive to these factors and the reference model has also been constructed according to the geometry of the PMK facility. Therefore, it has been decided to show the effect of the previously mentioned, so called 'efficiency factor' of the hydroaccumulators.

## 5.1 RELAP5 Results

The modifications of the RELAP5 model are listed in Table 5-1, while the comparison between the two applied geometries can be seen in Figure 5-1, where the 'A' part refers to the modified geometry (applied in the reference and *Dc* models), while 'B' is the real one (*Geom*, *Geom\_Dc*). In advance, we can conclude, that the (5%) modification of the break discharge coefficient has a minor effect on the characteristics of the main processes; therefore, we sometimes refer to the calculations as case A and case B, grouping *Base* & *Dc* and *Geom* & *Geom\_Dc*, respectively.

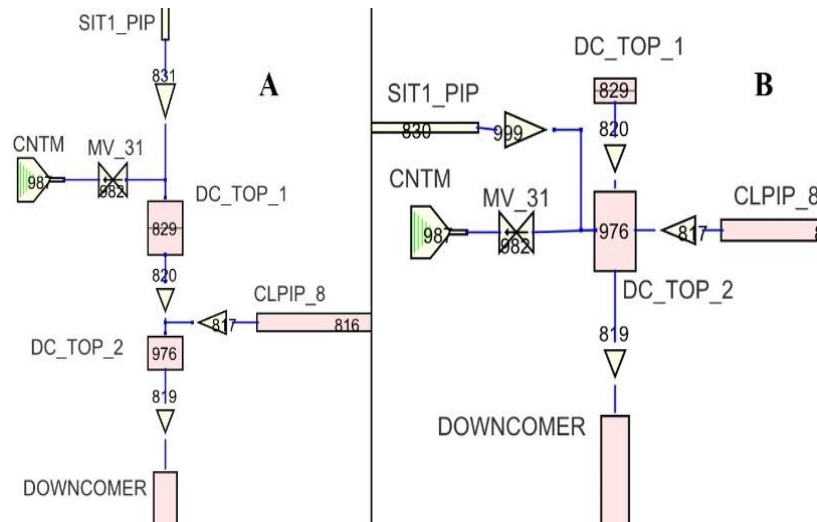


**Figure 5-1 DC Top Region Modeling – RELAP5**

It can be seen, that in case 'A' both the break and SIT1 surge line are connected to the DC top at a slightly higher elevation. As a result, the DC\_TOP\_1 part is more directly involved in the processes. In the models considering the real geometry (case 'B'), more of the water flowing through the cold leg, and less of the accumulator's cold water is discharged through the break valve (compared to those of case 'A'), due to the proximity of these connections. This mainly affects the initial phase of the transient, when the HAs are already injecting into the system (~50-110 s), as the primary pressure (Figure 5-2) drops well below of that of the measurement (and the *Base* model). Therefore, the hydroaccumulator water level (Figure 5-3) is also lower in this stage. Then, the injection practically stops for around 150 seconds, which delays its further emptying. Meanwhile, a strong boiling process was observed in the DC top region in case 'B', which among others resulted in an early decrease of the DC coolant level (Figure 5-4) and lower break mass flow rates (compared to that of the *Base* - Figure 5-5).

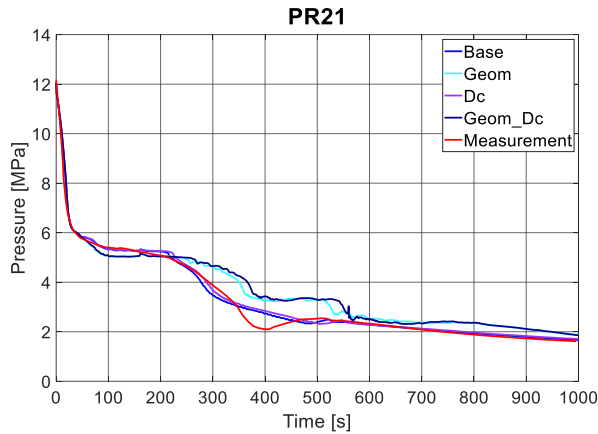


**Figure 5-2 Primary Pressure  
– RELAP5 Calculations**

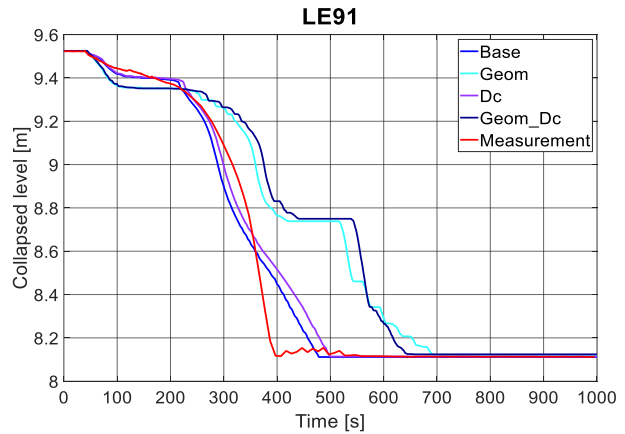


**Figure 5-3 HA1 Coolant Level  
– RELAP5 Calculations**

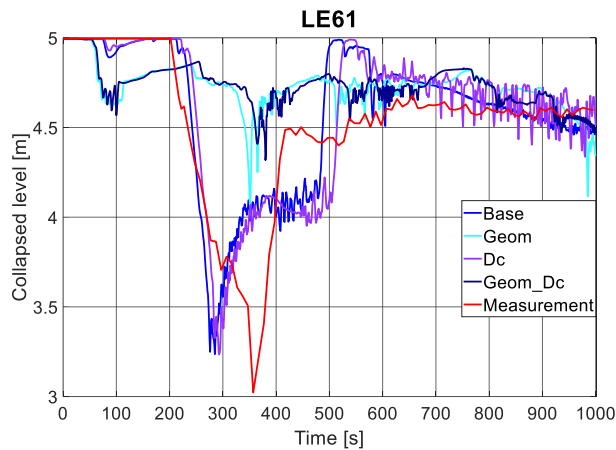


**Figure 5-4 DC Coolant Level  
– RELAP5 Calculations**

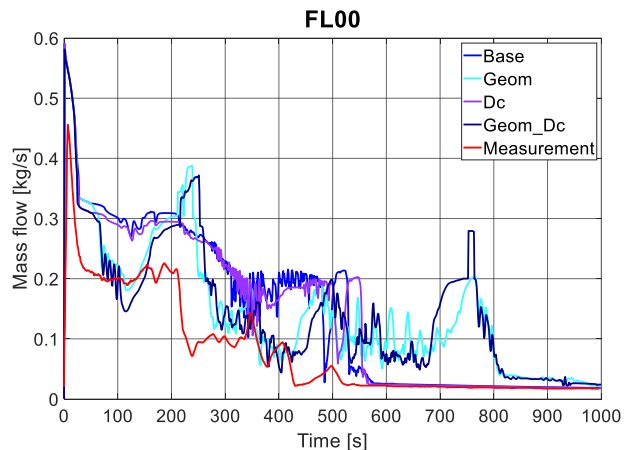


**Figure 5-5 Mixture Mass Flow of the  
Break Valve  
– RELAP5 Calculations**

As the mass of the total leaked coolant, based on Figure 5-5 and Figure 5-6 (RPV coolant level), is significantly less in *Geom* and *Geom\_Dc* models, the first clearance of the loop seals is also delayed. When the trapped steam reaches the break area, the depressurization of the primary system continues, allowing the further injection of the accumulators. This again, results in a delayed HL loop seal refilling (compared to the reference calculation), but in these cases (*Geom*, *Geom\_Dc*), the timing (compared to the measurement) is pretty accurate (Figure 5-7). This is followed once again by a stagnating period (roughly between 400 and 500 s), which ends when the temporal loop seal clearing (at around 500 s) allows the steam passing through the piping. Once the pressure drops again, the restarted rapid accumulator injection provides enough ECCS water to significantly raise the RPV level and to refill the loop seal approximately for another 200 s.

As the discharge of the primary coolant continued, the final loop seal clearance took place at around 750 s. Meanwhile the HA injection terminated and due to the still relatively high break mass flow rate and the continuous HPIS injection, approximately the same RPV water level remained in the RPV for the last 3 minutes of the transient.

The behaviour of the secondary side (see Figure 5-8) is only moderately affected by the applied modifications. It can be seen that the further decrease of the upper plenum pressure (below 5 MPa) in case B results in lower secondary pressures in the first stage. The trend flips however, as the primary pressure stays well above that of the measurement (and the *Base* case) throughout the rest of transient, leading to a slower depressurization rate of the secondary side.

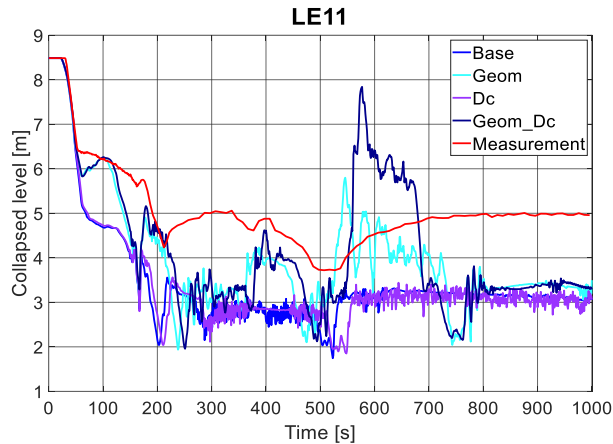


**Figure 5-6 RPV Coolant Level – RELAP5 Calculations**

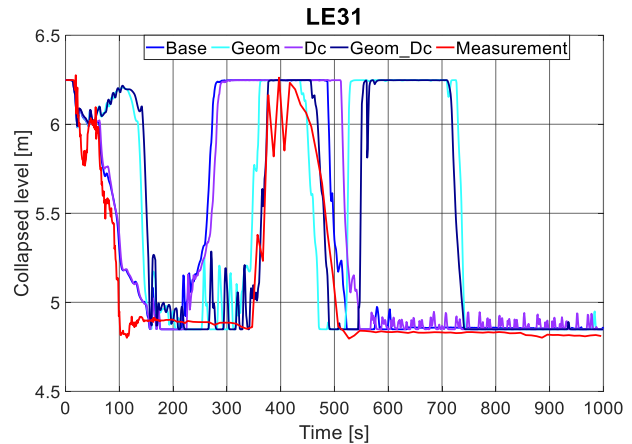


**Figure 5-7 HL Loop-Seal Level – RELAP5 Calculations**

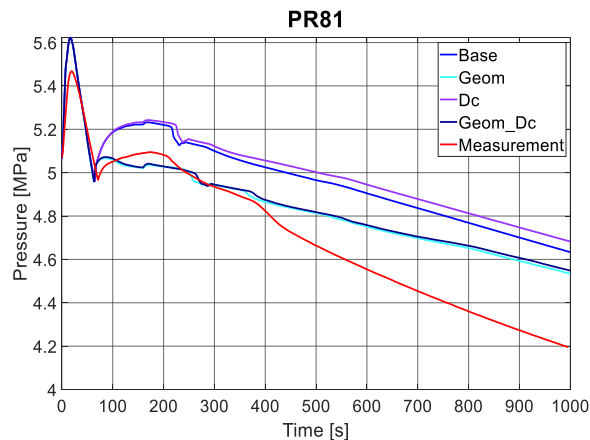


**Figure 5-8 Secondary Pressure – RELAP5 Calculations**

As a conclusion of this section, the RELAP5 model of the SPE-2 experiment tends to be overly sensitive on the positioning of the DC\_TOP connections, while the effect of the discharge coefficient itself is much smoother, since its modification, as expected, did not change significantly the main characteristics of the transient.



## 5.2 TRACE Results

As mentioned earlier, the TRACE model has also undergone a geometrical modification of the DC top connections throughout the development stage. The layout of the *Base* and the *Geom* models are illustrated as 'A' and 'B' in Figure 5-9, respectively. Unlike the RELAP5 model, only the accumulator outlet junction had been placed to a slightly higher elevation this time (compared to the original geometry of the facility).

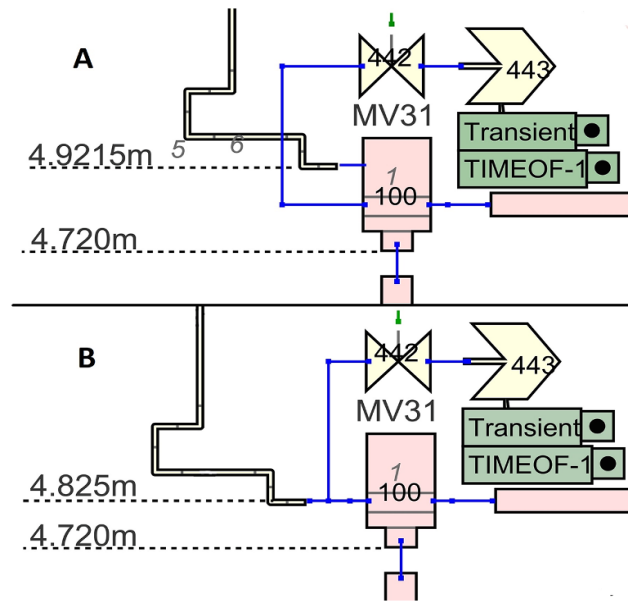


**Figure 5-9 DC Top Region Modeling – TRACE**

The overall simulation results presented by the following figures again indicate, that the *Dc* curves are closer in nature to those of the *Base*. It has to be highlighted however, that in case of the TRACE sensitivity analysis, only an adjustment of 1% has been applied on the discharge coefficient (see Table 3-1). While the single-phase outflow stage is, as expected, not affected by this modification, the later phases show some discrepancies in the results.

In case of the hot leg loop seal (*Dc* version, Figure 5-10), no such temporary emptying processes can be observed during its refilling period as in the *Base* one. As these introduced a 'delay' required for the right timing of the complete refill, the *Dc* model predicts it approximately 100 s earlier. As a result, higher upper plenum pressure (Figure 5-11) can be observed in this phase, which also causes slightly slower HA injection rates (Figure 5-12). This simulation, furthermore, shows slightly lower coolant level drops both in the RPV (Figure 5-13) and the downcomer (Figure 5-14).

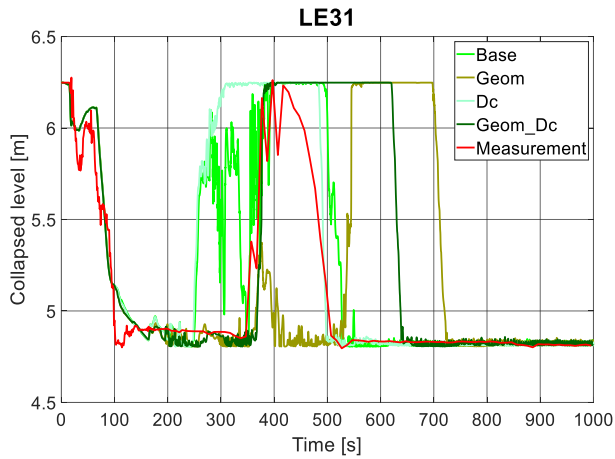


**Figure 5-10 HL Loop-Seal Level  
– TRACE Calculations**

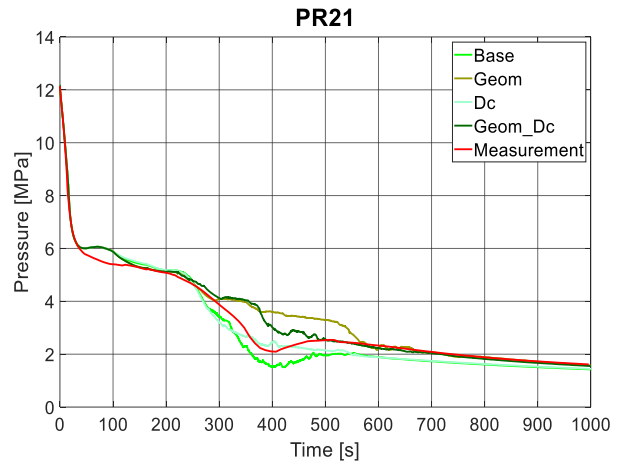


**Figure 5-11 Primary Pressure  
– TRACE Calculations**

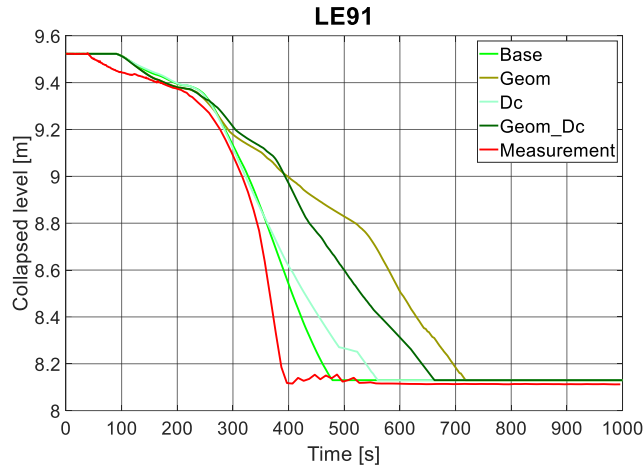


**Figure 5-12 HA1 Coolant Level – TRACE Calculations**

Due to the significantly lower break mass flows (Figure 5-15) observed in the first half of the transient, the coolant inventory (Figure 5-13 & Figure 5-14), in these simulations is mostly higher compared to that of the *Base* case. The timing of the loop seal behavior is also shifted Figure 5-10. It is worth mentioning however, that, most likely better overall agreement could have been reached if the discharge coefficient was further adjusted to the actual (*Geom*) model.

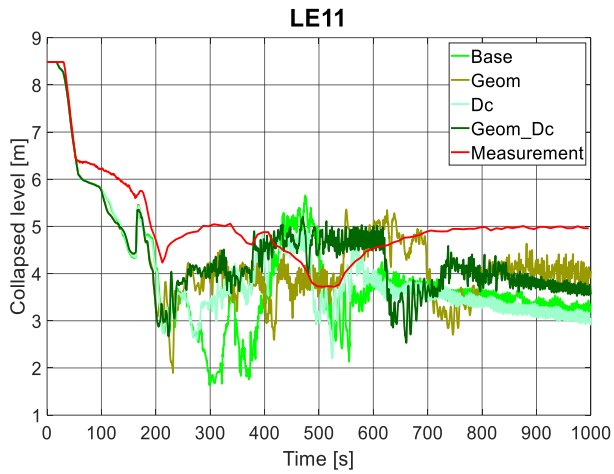


**Figure 5-13 RPV Coolant Level – TRACE Calculations**

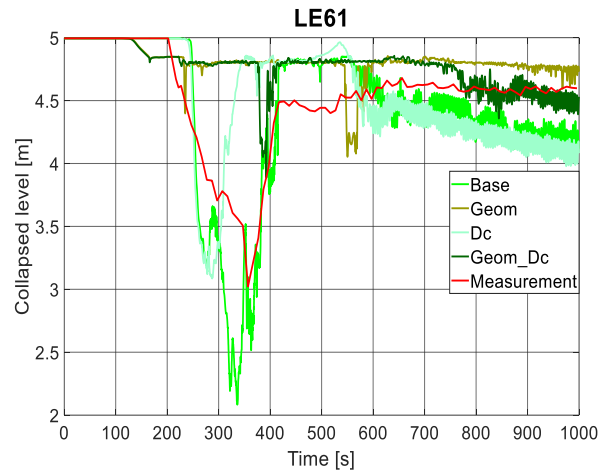


**Figure 5-14 DC Coolant Level – TRACE Calculations**

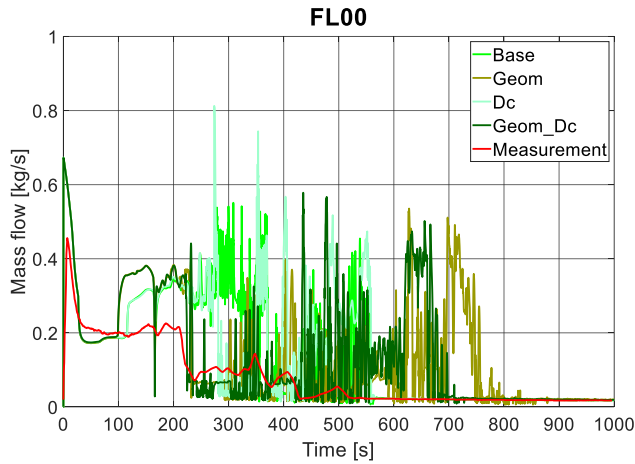


**Figure 5-15 Mixture Mass Flow of the Break Valve – TRACE Calculations**

### 5.3 APROS Results

According to our research, APROS have not appeared to be as sensitive on the modelling of the top of the downcomer region as the other two codes. Therefore, this section focuses on an APROS-specific parameter, the setting of which is crucial for such calculations. Our previous studies carried out with APROS in the Institute revealed, that the built-in ACCUMULATOR component of APROS does not handle the interfacial heat transfer properly in some cases with the default settings. In order to overcome this issue, the modification of the so-called 'efficiency factor' of the interfacial heat transfer proved to be the solution multiple times in the past [2], [12].

In the APROS model evaluated in the previous chapter (denoted as '*Modified\_HA*' from now on), an efficiency parameter of 3.5 and 3.0 has been set to accumulators 1 and 2, respectively. For comparison, the value of 5.0 was used for both in the SPE-4 experiment [1]. In this section, we would like to briefly show the effect of leaving the efficiency parameter on its default value (1.0) on the results (*Default\_HA*).

In the first ~ 250 s, the main trends of the system are preserved also in *Default\_HA*, however, in the model (due to the underestimated interfacial HT) the gas temperature of the HA would decrease below 0 degrees Celsius, which the code cannot interpret. Consequently, the temperature is held above freezing point and much lower injection rates can be observed (Figure 5-16).

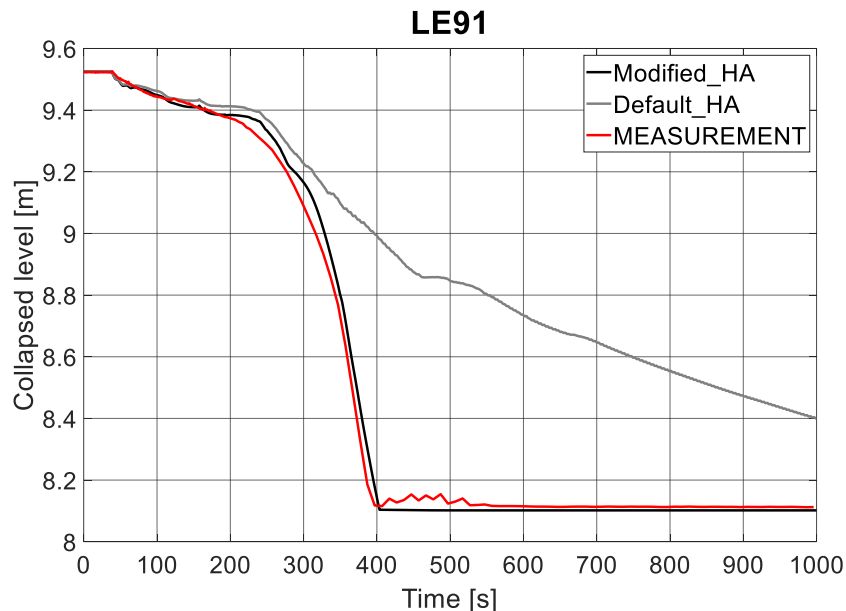


**Figure 5-16 HA1 Coolant Level – APROS Calculations**

Moreover, the depressurization rate of the primary side (Figure 5-17) after 330 s is underpredicted and the SITs fail to refill the HL loop seal (Figure 5-18). Thus, there is no rising period of the primary pressure around between 400 and 500 s. Towards the end of the transient, the sufficient cooling is not maintained for the heater rods due to the lack of inventory, which, in the long run would result in a fuel rod dry-out (Figure 5-19).

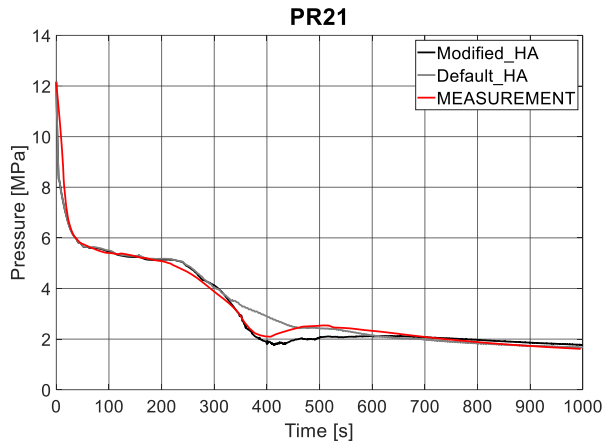


**Figure 5-17 Primary Pressure  
– APROS Calculations**

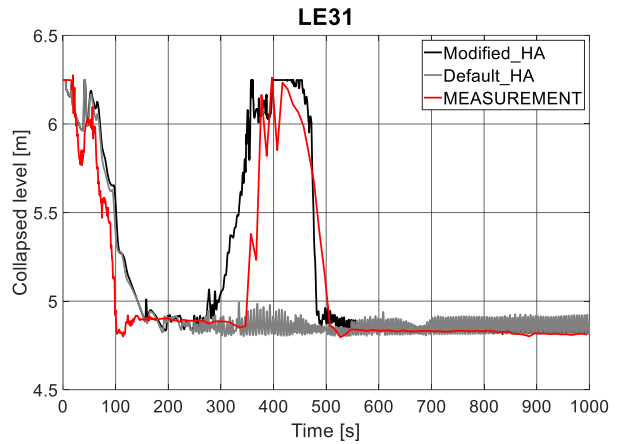


**Figure 5-18 HL Loop-Seal Level  
– APROS Calculations**

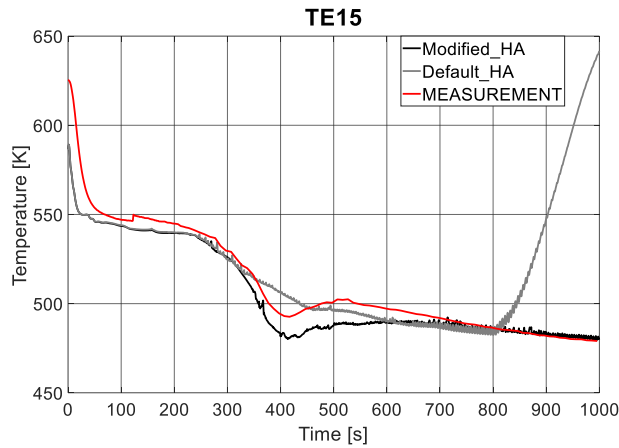


**Figure 5-19 Heater Rod Cladding Temperature – APROS Calculations**

As a conclusion, we can affirm, that choosing the appropriate 'efficiency factor' is of fundamental importance when investigating transients of test facilities. Since the APROS code has been built mainly to simulate full-plant behaviour, those cases may be better predicted with the default accumulator settings.



## 6 QUANTITATIVE EVALUATION OF THE MODELS

Similarly to our previous CAMP agreement report [1] dealing with the SPE-4 experiment, the FFTBM-SM and SARBM methods were used as tools for the objective assessment of the calculations. For the overview of the fundamentals of these techniques we advise the reader to refer to [1], [13]. Here, we only introduce the accuracy measures used in the following sections.

In case of FFTBM-SM, the average amplitude ( $AA_m$ ) is used, as the main indicator of the calculation accuracy for a given parameter. After all the relevant variables are chosen by the user for the evaluation, the so called total average amplitude ( $AA_{m,tot}$ ) is being calculated, through the recommended weighting factors (WF) for the different categories: e.g. pressure, water level, temperature signals. Then, based on Table 6-1 one can classify the performance of single parameters (single  $AA_m$  values) or the overall calculation ( $AA_{m,tot}$ ).

Due to its special importance, a much stricter criterion of  $AA_m < 0.1$  has been proposed for the primary pressure in case of the original FFTBM. When the improved version of this method (FFTBM-SM – FFTBM with signal mirroring) has been introduced [14], the same acceptability criteria has been applied, however, the calculated average amplitude values increased moderately (compared to the ones given by the original FFTBM), which made this target even harder to reach. Based on our previous study [1], therefore, the K value of 0.2 has been proposed for the primary pressure.

**Table 6-1 Accuracy Categories of FFTBM and SARBM [15]**

Category	FFTBM(-SM)	SARBM
acceptable	$AA_m, AA_{m,tot} \leq K = 0.4$	$AF_{tot} \leq K = 0.2$
very good	$AA_m, AA_{m,tot} \leq 0.3$	$AF_{tot} \leq 0.1$
good	$0.3 < AA_m, AA_{m,tot} \leq 0.5$	$0.1 < AF_{tot} \leq 0.25$
poor	$0.5 < AA_m, AA_{m,tot} \leq 0.7$	$0.25 < AF_{tot} \leq 0.45$
very poor	$0.7 < AA_m, AA_{m,tot}$	$0.45 < AF_{tot}$

Considering SARBM method, the behaviour of the so-called AF (accuracy factor) is the closest to that of the AA-s in case of the FFTBM-SM (the lower the value, the higher the accuracy), so these are the most widely used. In addition, similar categories can be defined for SARBM evaluation, which we have also listed in Table 6-1.

### 6.1 Handling of Reference Water Levels in the Quantitative Methods

In the current quantitative assessment, 17 variables were taken into consideration, which are listed in Table 6-2. In order to be consistent with the SPE-4 study [1], practically the same set of parameters was used here.

**Table 6-2 Parameter Set for the Quantitative Methods**

	Heated section differential pressure
DP41	SG differential pressure
FL01	Break valve mass flow
FL51	CL mass flow (upstream the HPIS)
LE11	RPV coolant level
LE31	HL loop-seal level
LE46	CL loop-seal level
LE61	DC coolant level
LE92	HA 2 water level
PR21	Upper plenum pressure
PR81	SG (secondary side) pressure
PR92	HA 2 pressure
TE15	Fuel rod cladding temperature
TE22	Upper head temperature
TE41	SG hot collector inlet temperature
TE42	SG cold collector outlet temperature
TE63	Lower plenum coolant temperature

When interpreting the output of the FFTBM-SM and SARBM however, a rather unexpected behaviour has been observed. It has been seen in the qualitative analysis, that most of the alternative model versions (except the *Dc* models in RELAP5 and TRACE) predict significantly lower accumulator injection rates throughout the transient, therefore the SIT water levels remain higher until the emptying (see Figure 5-3, Figure 5-12 and Figure 5-16). Based on these graphs one might expect that this behaviour would significantly worsen the values of the accuracy measures for the given variable (LE92). The *Default\_HA* model of APROS could, for example, certainly not be accepted.

Table 6-3 shows the  $AA_m$ -s and AF-s calculated for the HA water levels for two different model versions in each case (*Base & Geom* in case of RELAP5 and TRACE and *HA\_mod & HA\_def* for APROS).

It can be seen that all of the values indicate extremely high accuracy (see Table 6-1), which is clearly not the case (especially in the alternative model versions). According to our research, this rather inconsistent behaviour stems from the intrinsic characteristics of the FFTBM-SM and SARBM methods and draws attention to the correct input preparation for such calculations.

**Table 6-3 Accuracy Measures for SIT2 Water Level Calculations**

LE92	RELAP5	TRACE	APROS
$AA_{m, Base}, AA_{m, HA\_mod}$	0.030	0.019	0.015
$AA_{m, Geom}, AA_{m, HA\_def}$	0.055	0.080	0.078
$AF_{Base}, AF_{HA\_mod}$	0.005	0.003	0.002
$AF_{Geom}, AF_{HA\_def}$	0.015	0.024	0.026

We found out, that from the quantitative analysis point-of-view (in case of FFTBM-SM and SARBM), the selection of the lower limit (reference) of the range the code takes into account in the calculation for a given variable is of significant importance. The measured values of the experiment were mostly documented on a base of what we call ‘absolute levels’, i.e., the reference point for pressure, temperature and water level measurements was zero. The



distortion of this is barely noticeable for most of the signals, as their variation covers most of the range taken into account. The situation changes however, when we consider water levels, such as LE92 or LE31, where the range of possible changes is much narrower as the value of the signal cannot decrease under a specific level (e.g., measurement gauge elevation). In these cases, the denominator part, which is responsible for the normalization of the difference between the measured and calculated signal, is much larger compared to the difference itself. Hence, the output value decreases significantly and the users, who are unaware of this behaviour, could draw false conclusions based on the results. This issue should also be addressed in case of transients, during which the relative change of some variables is rather small in order to get consistent results.

Hereafter, we apply such alternative reference points for all the water level measurements and the accuracy measures calculated with these will be referenced to as 'relative' level type. For comparison we also list the same accuracy measures but calculated with zero reference, as a base, and they will be denoted as 'absolute' level type.

In Table 6-4 and Table 6-5 we listed all the water level measurements (considered in the quantitative analysis) and their respective accuracy measures calculated with both 'absolute' and 'relative' reference points. The same model versions were listed as in Table 6-3.

**Table 6-4 FFTBM-SM Quantification of Water Level Measurements based on 'Absolute' and 'Relative' Reference Points**

Meas.	Reference point	TRACE		RELAP5		APROS	
		$AA_{m, Base}$	$AA_{m, Geom}$	$AA_{m, Base}$	$AA_{m, Geom}$	$AA_{m, HA_{mod}}$	$AA_{m, HA_{def}}$
LE11	absolute	0.742	0.651	0.639	0.876	0.841	0.767
	relative	0.757	0.664	0.651	0.894	0.857	0.782
LE31	absolute	0.363	0.540	0.403	0.643	0.296	0.365
	relative	0.902	1.342	1.001	1.598	0.736	0.906
LE46	absolute	0.290	0.213	0.351	0.313	0.270	0.252
	relative	0.383	0.280	0.463	0.414	0.356	0.332
LE61	absolute	0.448	0.418	0.287	0.394	0.497	0.426
	relative	0.461	0.429	0.295	0.405	0.512	0.438
LE92	absolute	0.019	0.080	0.030	0.055	0.015	0.078
	relative	0.165	0.706	0.263	0.488	0.130	0.682
Total	absolute	0.222	0.265	0.179	0.238	0.215	0.226
	relative	0.249	0.315	0.211	0.289	0.237	0.268

Both tables show that the usage of relative water levels worsened the results, which is in line with the expectations. The biggest differences can be seen in case of LE92 and LE31 values, where the new measures indicate 'poor' or 'very poor' accuracies for the alternative model

versions. In the other 3 cases, a rather moderate discrepancy can be seen between the calculations with the original and new reference bases, as the signals vary along the whole range they can possibly cover [0, max] throughout the transient.

**Table 6-5 SARBM Quantification of Water Level Measurements based on ‘Absolute’ and ‘Relative’ Reference Points**

Meas.	Reference point	TRACE		RELAP5		APROS	
		AF <sub>Base</sub>	AF <sub>Geom</sub>	AF <sub>Base</sub>	AF <sub>Geom</sub>	AF <sub>HA_mod</sub>	AF <sub>HA_def</sub>
LE11	absolute	0.274	0.188	0.347	0.265	0.303	0.374
	relative	0.284	0.195	0.361	0.275	0.314	0.387
LE31	absolute	0.056	0.128	0.084	0.133	0.043	0.079
	relative	0.420	0.801	0.561	0.743	0.346	0.682
LE46	absolute	0.080	0.067	0.118	0.090	0.070	0.066
	relative	0.153	0.130	0.232	0.172	0.132	0.125
LE61	absolute	0.076	0.102	0.057	0.091	0.102	0.129
	relative	0.079	0.106	0.060	0.095	0.107	0.134
LE92	absolute	0.003	0.024	0.005	0.015	0.002	0.026
	relative	0.066	0.443	0.126	0.307	0.053	0.487
Total	absolute	0.068	0.086	0.061	0.077	0.061	0.077
	relative	0.085	0.125	0.085	0.110	0.076	0.115

An additional inconsistency must be noticed when using the newly proposed level type. In case of the hot leg loop seal level measurement, even the base models (*Base*, *HA\_mod*) are now categorized as ‘poor’ or worse by both quantitative methods, while we found their accuracies satisfactory in the qualitative evaluation. Despite the APROS calculation predicts characteristics of the loop seal processes accurately in the qualitative manner, for example, it is labelled as ‘very poor’ and ‘poor’ by FFTBM-SM and SARBM, respectively. The reason behind this observation could be the fact, that a relatively narrow range of the parameter change is considered (approx. 1.5 m), the limits of which are reached multiple times (loop seal clearing and refilling processes) during the evolution of the transient. Because of this, the discrepancies of the timing of the quick trend changes become overly amplified by the methods. We would recommend further investigation on this behaviour in order to better understand and handle such situations.

## 6.2 Evaluation of the Alternative Model Versions

Table 6-6 lists the total accuracy measures of both methods (considering the newly proposed references) for each model version introduced in the sensitivity analysis. Based on these values it can be concluded that each of the main models fall under the ‘very good’ category, even when using the so-called relative water levels. Moreover, the results show, that the overall accuracy of those alternative models is still within the acceptable range, but in most cases, as expected, clearly worse than that of the *Base* (or *Modified\_HA* in APROS). The only exception can be seen when comparing *Base* and *Dc* models of TRACE. In this case, FFTBM-SM considers the *Dc* version, as the more accurate one, however, based on the qualitative assessment we believe the *Base* model predicts the processes more accurately.

**Table 6-6 Comparison of Total Accuracies between the Codes and Alternatives (Relative Reference Points)**

Code	Model Version	AF <sub>tot</sub>	AA <sub>m, tot</sub>
RELAP5	<b>Base</b>	<b>0.085</b>	<b>0.211</b>
	<i>Dc</i>	0.086	0.220
	<i>Geom</i>	0.110	0.289
	<i>Geom_Dc</i>	0.115	0.302
TRACE	<b>Base</b>	<b>0.085</b>	<b>0.249</b>
	<i>Dc</i>	0.085	0.233
	<i>Geom</i>	0.125	0.315
	<i>Geom_Dc</i>	0.102	0.278
APROS	<b>Modified_HA</b>	<b>0.076</b>	<b>0.237</b>
	<i>Default_HA</i>	0.115	0.268

In addition to the analysis of the general AA<sub>m, tot</sub> and AF<sub>tot</sub> values, we also examined the specific primary pressure criterion, since it plays a prominent role in the processes. These values are summarized in Table 6-7.

**Table 6-7 Primary Pressure Accuracies for Base Models**

	RELAP5	TRACE	APROS
AA <sub>m, PR21</sub>	0.172	0.177	0.375
AF <sub>PR21</sub>	0.057	0.108	0.087

It can be seen that the strict criterion of the original FFTBM could not be reached in any of the codes, however, our RELAP5 and TRACE models fulfil the recently proposed target of  $AA_{m, PR21} \leq 0.2$ . On the other hand, contrary to the observations of the qualitative analysis, where APROS seemed to be the most accurate predicting the primary pressure evolution, FFTBM-SM evaluated it as the worse with a significantly higher average amplitude value than the other two. We will try to determine the reason behind this behaviour in the followings.

For this purpose, we took advantage of an extremely useful function of the FFTBM and SARBM, which allows to plot the evolution of the  $AA_m$ -s for a chosen variable during a specified timeframe. With such graphs, one can track the accumulation of the  $AA_m$ -s and AF-s, and point those phases, which are the biggest contributors for the increment. In the current study, we have divided the (~1000 s long) transient into 25 smaller intervals of nearly equal size and investigated the total and the UP pressure accuracy measures.

In Figure 6-1 and Figure 6-2, the time-dependent primary pressure  $AA_m$ -s and AF-s are shown for our base cases. These curves indicate clearly, that the APROS calculation accumulated the most inaccuracies in the first 40 seconds, during which the depressurization rate is overestimated by the base calculation (see Figure 4-1). After this stage, the FFTBM measure increased only to a minor extent, while the AF value (due to SARBM's different characteristics) even decreased below 0.1, which would indicate a 'very good' match. Nevertheless, despite the inaccuracy indicated by FFTBM-SM, the APROS calculation was capable of addressing the major processes and their timings (as seen in the previous sections), and it only failed to reproduce the early depressurization phase.

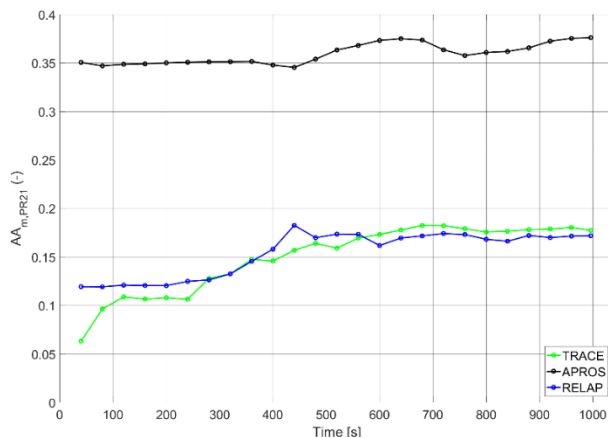


**Figure 6-1 Time-Dependent Accuracy of the UP Pressure (FFTBM-SM)**

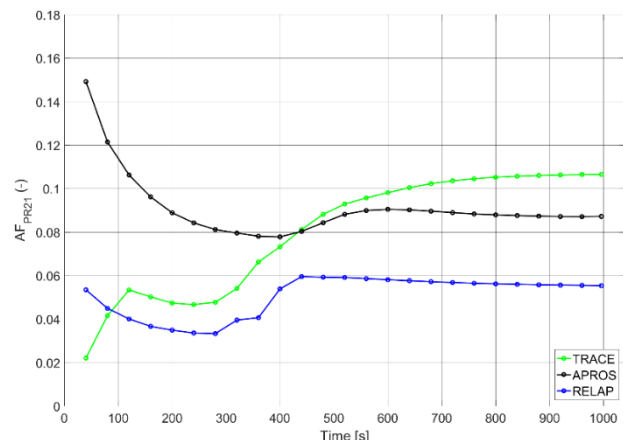


**Figure 6-2 Time-Dependent Accuracy of the UP Pressure (SARBM)**

Furthermore, the evolution of the total accuracy measures on Figure 6-3 and Figure 6-4 confirms our observations about the transient (see at Chapter 4). Both graphs show that the very beginning of the transient and the middle stages, where numerous complex processes take place at the same time, is the hardest to predict accurately. This is indicated by the elevated rate of the inaccuracy accumulation in the first 40 s and between around 200 and 450 s. Despite the UP pressure is an important contributor to these values, the curves of APROS show, that the calculation in general is of similar accuracy than RELAP5 and TRACE. Therefore, we would also consider it as a qualified model for the transient under investigation.

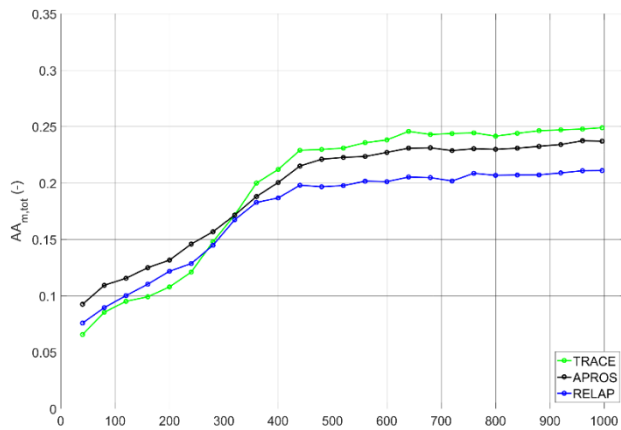


**Figure 6-3 Time-Dependent Total Accuracy of the Base Calculations (FFTBM-SM)**

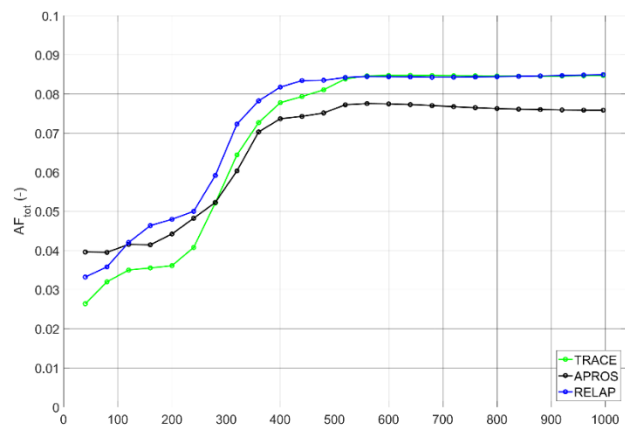


**Figure 6-4 Time-Dependent Total Accuracy of the Base Calculations (SARBM)**

At last, we compare the time-dependent total average amplitudes of the alternative models to those of the base one's. This step again helps to highlight those parts of the transient, in which the alternative versions perform worse.

As mentioned earlier, both RELAP5 and TRACE are very sensitive on the geometrical modifications of the DC top connections. While TRACE (Figure 6-5) tends to be quite sensitive on altering (1%) the two-phase discharge coefficient, RELAP5 (Figure 6-6) calculation pairs (*Base & Dc* and *Geom & Geom\_Dc*) show smaller discrepancies, even though a 5% modification has been applied in those cases. Also, the graphs of RELAP5 indicate, that the behaviour of these pairs of calculations is significantly different, as the difference in inaccuracy accumulation is rather continuous throughout the whole transient. On the other hand, the discrepancy between those curves of the TRACE calculations arises in the second part of the transient (after 420 s), which indicates mainly, that the modelling of the final loop seal clearance and the end of the accumulator injection rates are unacceptable in those cases.

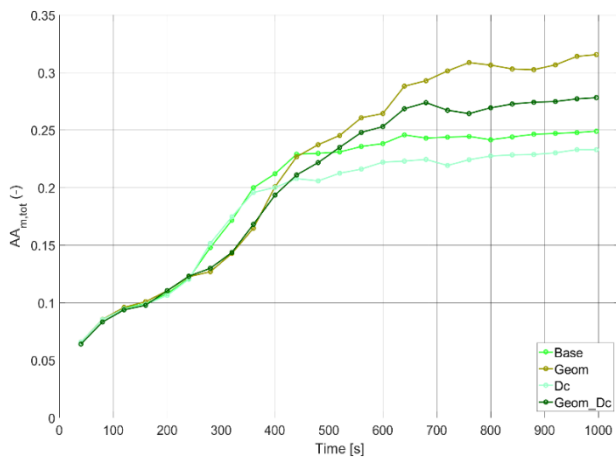


**Figure 6-5 Time-Dependent Total Average Accuracy of the Alternative TRACE Model Versions**

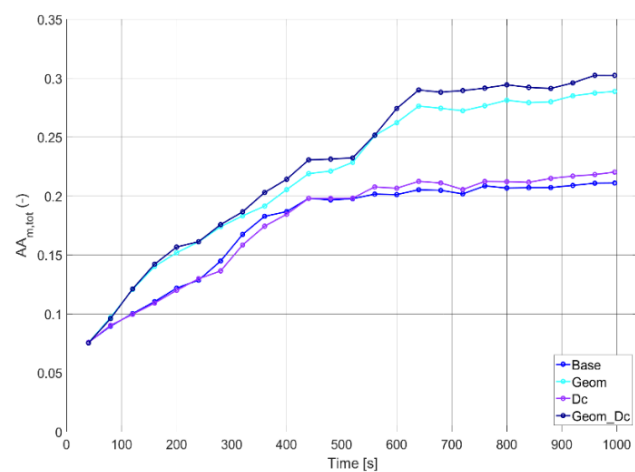


**Figure 6-6 Time-Dependent Total Average Accuracy of the Alternative RELAP5 Model Versions**

As seen in Figure 6-7, the time-dependent average amplitude evolution in the two investigated APROS models are quite similar. The qualitative evaluation revealed some major discrepancies, especially in the SIT injection rates, loop-seal behaviour and at the end of the transient the partial uncovering of the heater rods in the *Default\_HA* model. These variables, however, only seem to have moderate effect on the total  $AA_m$  and the relatively good accuracy of the other parameters (listed in Table 6-2) taken into consideration with the appropriate WFs [15] are compensating for these rather significant errors.

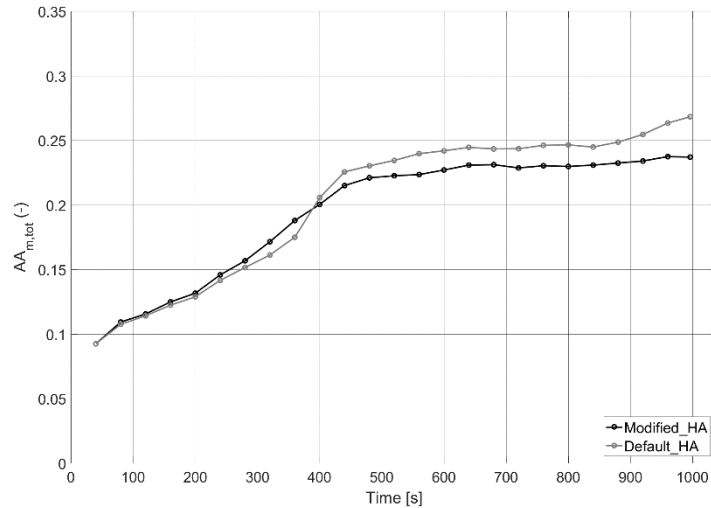


**Figure 6-7 Time-Dependent Total Average Accuracy of the Alternative APROS Model Versions**

These methods again, supported by the qualitative assessment, proved to be powerful tools for quantifying code prediction capability. In general, the qualitative and quantitative analysis drew the same conclusions, however some cases require the combination and comparison of these in order to better understand the behaviour of the system. The influence of the initial upper plenum pressure in APROS calculation (*Modified\_HA*) on the overall PR21 accuracy could be mentioned, as the best example in this regard.

Our observation about the sensitivity of the connection elevations in the DC top region has been also proven by the FFTBM-SM and SARBM, as those geometrically modified model variants are labelled as less accurate. Nevertheless, the accuracy measures of these alternative models suggest better agreement with the measurements than expected, based on the qualitative analysis in Chapter 5.

## 7 SUMMARY

This report deals with the second Standard Problem Exercise carried out on the PMK-2 integral test facility. In this experiment, a DBA scenario was investigated, featuring a CL small-break LOCA, with the availability of a single HPIS and two SITs.

A former study of ours was dealing with the SPE-4 exercise, for which we have developed qualified RELAP5, TRACE and APROS models [1] [2]. We have successfully modified these models in order to address the SPE-2 transient [3]. Throughout the model development it turned out, that the modelling of the downcomer top region is crucial, as numerous lines (including the break, SIT2 surgeline) are connected to a relatively small volume resulting in processes with high degree of complexity. Our RELAP5 and TRACE models also required a minor rearrangement of these connections in this region in order to produce the best results.

Besides the qualitative evaluation of the simulation results, a quantitative assessment has been performed with FFTBM-SM and SARBM. In [1] we have already proposed a more permissive primary pressure criterion for FFTBM-SM. Considering this criterion the quantitative assessment showed, that both RELAP5 and TRACE models fulfil all the requirements to be considered as adequate. On the other hand, the APROS calculation failed to fulfil the criterion for the primary pressure, as the rate of the initial pressure drop has been overestimated by the code. In spite of this, the APROS simulation captured the main processes very well, which is also indicated by its overall accuracy measures. We have also drawn attention to a potential user error regarding the considered reference level of the measurements signals in FFTBM-SM and SARBM, which could give misleading results (in a non-conservative way) in certain cases.

Furthermore, a small-scale sensitivity analysis has been performed, in which altogether 7 alternative model versions were introduced. The detailed comparison of these to the original models uncovered their weaknesses and showed the sensitivity of the base models to different modifications.





## 8 REFERENCES

- [1] R.Orosz, T. Varju, Á. Aranyosy, V. Holl, T. Hajas & A. Aszódi , 2022. RELAP5, TRACE and APROS Model Benchmark for the IAEA SPE-4 Experiment (NUREG/IA-0533)
- [2] Varju, T., Aranyosy, Á., Orosz, R., Holl, V., Hajas, T., Aszódi, A., 2021. Analysis of the IAEA SPE-4 small-break LOCA experiment with RELAP5, TRACE and APROS system codes, Nuclear Engineering and Design, Volume 377, 111109, June 2021. (<https://doi.org/10.1016/j.nucengdes.2021.111109>)
- [3] Varju, T., Orosz, R., Aranyosy, Á., Holl, V., Hajas, T., Aszódi, A., 2022. Sensitivity analysis of the IAEA SPE-2 small-break LOCA experiment with RELAP5, TRACE and APROS system codes, Nuclear Engineering and Design, Volume 388, 111630, March 2022. (<https://doi.org/10.1016/j.nucengdes.2021.111630>)
- [4] Parzer, I., Mavko, B., Petelin, S., 1992. An overview analysis of IAEA standard problem exercises
- [5] Mavko, B., Parzer, I., Petelin, S., 1994. A modeling study of the PMK-NVH integral test facility
- [6] Galetti, M.R.S., Madeira, A.A., Borges, R.C., Pontedeiro, A.C., 1990. Post-test analysis of SPE-2 with TRAC-PF1 (IAEA-TC--56003). International Atomic Energy Agency (IAEA)
- [7] Bánáti, J., 1995. Assessment of RELAP5/MOD3.1 code for the IAEA SPE-4 experiment, ASME/JSME Fluids Engineering and Laser Anemometry Conference and Exhibition, August 13-18, 1995, Hilton Head Island, South Carolina. Vol. 223.
- [8] Parzer, I., 2003. Break Model Comparison In Different RELAP5 Versions, Nuclear Energy for New Europe 2003, Portorož, Slovenia
- [9] IAEA-TECDOC-477: Simulation of a loss of coolant accident with hydroaccumulator injection, Vienna, 1988.
- [10] IAEA-TECDOC-848: Simulation of a loss of coolant accident without high pressure injection but with secondary side bleed and feed, Vienna, 1995.
- [11] L. Szabados, Gy. Ézsöl L. Pernecky, I Tóth: Results of the Experiments Performed in the PMK-2 Facility for VVER safety studies, Budapest, 2007.
- [12] Kauppinen, O.-P., Kouhia, V., Riikonen, V., Hyvärinen, J., 2019. System code analysis of accumulator nitrogen discharge during LOCA experiment at PWR PACTEL test facility, Nuclear Engineering and Design, Volume 353, 2019, 110288, ISSN 0029-5493.
- [13] Leonardi, M., D’Auria, F., Pochard, R., 1994. Methodology for the evaluation of thermohydraulic codes accuracy. Proceedings of “New trends in Nuclear System Thermohydraulics” Conference, Pisa May 30-June 2, 1994.
- [14] Prošek, A., 2002. Lessons learned from accuracy assessment of IAEA-SPE-4 experiment predictions. Nuclear Energy for New Europe 2002 (International Conference), Kranjska Gora, Slovenia, September 9-12, 2002.

- [15] Bovalini, R., D'Auria, F., Leonardi, M., 1992. Qualification of the Fast Fourier Transform based methodology for the quantification of thermalhydraulic code accuracy. DCMN Report, NT 194 (92), Pisa, July 1992.

**BIBLIOGRAPHIC DATA SHEET**

(See instructions on the reverse)

**NUREG/IA-0544**

2. TITLE AND SUBTITLE

**RELAP5, TRACE and APROS Model Benchmark for the IAEA SPE-2  
Experiment**

3. DATE REPORT PUBLISHED

MONTH

**March**

YEAR

**2024**

4. FIN OR GRANT NUMBER

5. AUTHOR(S)

R. Orosz, T. Varju, Á. Aranyosy, V. Holl, T. Hajas & A. Aszódi

6. TYPE OF REPORT

7. PERIOD COVERED (Inclusive Dates)

Technical

8. PERFORMING ORGANIZATION - NAME AND ADDRESS (If NRC, provide Division, Office or Region, U. S. Nuclear Regulatory Commission, and mailing address; if contractor, provide name and mailing address.)

Budapest University of Technology and Economics  
Institute of Nuclear Techniques  
Műgyetem rkp. 3.  
1111 Budapest, Hungary

9. SPONSORING ORGANIZATION - NAME AND ADDRESS (If NRC, type "Same as above", if contractor, provide NRC Division, Office or Region, U. S. Nuclear Regulatory Commission, and mailing address.)

Division of Systems Analysis  
Office of Nuclear Regulatory Research  
U.S. Nuclear Regulatory Commission  
Washington, D.C. 20555-0001

10. SUPPLEMENTARY NOTES

K. Tien, NRC Project Manager

11. ABSTRACT (200 words or less)

In the recent decades, with the ever-growing computational capacity, system codes have become essential tools at research and development activities, assessments and licencing procedures of NPPs and research reactors. Among others, a broad literature of assessments performed with RELAP5 and TRACE codes is now available, proving the reliability of the produced results.

In one of our previous studies, dealing with the IAEA SPE-4 benchmark test, we evaluated and compared our simulation results of multiple system codes, namely RELAP5, TRACE and the Finnish APROS. The current study could be considered as the continuation of the mentioned one, as both tests were conducted on the PMK-2 integral test facility in Budapest, Hungary. Although both benchmarks are dealing with a CL-SBLOCA transient, there are several key differences greatly influencing the transient behaviour, such as the availability of emergency core cooling systems (ECCS) or the secondary side bleed and feed operation.

As there are significantly less studies dealing with this particular test and those available resulted, on average, in lower accuracy compared to those of the SPE-4, we decided to investigate it simultaneously with three system codes: RELAP5, TRACE and APROS. The results have been evaluated qualitatively and quantitatively through FFTBM and SARBM methods.

12. KEY WORDS/DESCRIPTORS (List words or phrases that will assist researchers in locating the report.)

PMK-2  
SPE-2  
RELAP5  
TRACE  
APROS  
VVER  
SBLOCA  
FFTBM-SM  
SARBM

13. AVAILABILITY STATEMENT

unlimited

14. SECURITY CLASSIFICATION

(This Page)

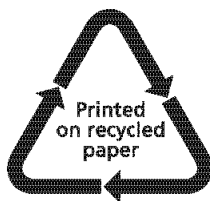
unclassified

(This Report)

unclassified

15. NUMBER OF PAGES

16. PRICE



Federal Recycling Program



**UNITED STATES  
NUCLEAR REGULATORY COMMISSION  
WASHINGTON, DC 20555-0001**

**OFFICIAL BUSINESS**



@NRCgov



**NUREG/IA-0544**

**RELAP5, TRACE and APROS Model Benchmark for the IAEA SPE-2 Experiment**

**March 2024**